G. Blasse · B. C. Grabmaier

LUMINESCENT MATERIALS

Springer-Verlag


ALLE ZEIT WACHT
1842

G. Blasse, B. C. Grabmaier

Luminescent Materials

With 171 Figures and 31 Tables

Springer-Verlag
Berlin Heidelberg New York
London Paris Tokyo
Hong Kong Barcelona Budapest

Prof. Dr. G. Blasse

Debye Institute
University Utrecht
Postbox 80.000
3508 TA Utrecht
The Netherlands

Prof. Dr. B. C. Grabmaier

Siemens Research Laboratories
ZFE BT MR 22
D-81730 München
Germany

also with Debye Institute
University Utrecht

ISBN 3-540-58019-0 Springer-Verlag Berlin Heidelberg New York
ISBN 0-387-58019-0 Springer-Verlag New York Berlin Heidelberg

Library of Congress Cataloging-in-Publication Data
Blasse, G. Luminescent materials / G. Blasse, B.C. Grabmaier. p. cm.
Includes bibliographical references and index.
ISBN 3-540-58019-0. -- ISBN 0-387-58019-0 (U.S.)
1. Phosphors. 2. Luminescence. I. Grabmaier, B. C., 1935- II. Title.
QC476.7.B53 1994 620.1'1295--dc20 94-20336 CIP

Printed in Germany

Typesetting with TEX: Data conversion by Lewis & Leins, Berlin
SPIN: 10187460 02/3020 - 5 4 3 2 1 0 - Printed on acid-free paper

Preface

Luminescence is just as fascinating and luminescent materials (are) just as important as the number of books on these topics are rare. We have met many beginners in these fields who have asked for a book introducing them to luminescence and its applications, without knowing the appropriate answer. Some very useful books are completely out of date, like the first ones from the late 1940s by Kröger, Leverenz and Pringsheim. Also those edited by Goldberg (1966) and Riehl (1971) can no longer be recommended as up-to-date introductions.

In the last decade a few books of excellent quality have appeared, but none of these can be considered as being a general introduction. Actually, we realize that it is very difficult to produce such a text in view of the multidisciplinary character of the field. Solid state physics, molecular spectroscopy, ligand field theory, inorganic chemistry, solid state and materials chemistry all have to be blended in the correct proportion.

Some authors have tried to obtain this mixture by producing multi-authored books consisting of chapters written by the specialists. We have undertaken the difficult task of producing a book based on our knowledge and experience, but written by one hand. All the disadvantages of such an approach have become clear to us. The way in which these were solved will probably not satisfy everybody. However, if this book inspires some of the investigators just entering this field, and if it teaches him or her how to find his way in research, our main aim will have been achieved.

The book consists of three parts, although this may not be clear from the table of contents. The first part (chapter 1) is a very general introduction to luminescence and luminescent materials for those who have no knowledge of this field at all. The second part (chapters 2-5) gives an overview of the theory. After bringing the luminescent center in the excited state (chapter 2: absorption), we follow the several possibilities of returning to the ground state (chapter 3: radiative return; chapter 4: nonradiative return; chapter 5: energy transfer and migration). The approach is kept as simple as possible. For extensive and mathematical treatments the reader should consult other books.

Part three consists of five chapters in which many of the applications are discussed, viz. lighting (chapter 6), cathode-ray tubes (chapter 7), X-ray phosphors and scintillators (chapters 8 and 9), and several other applications (chapter 10). These chapters discuss the luminescent materials which have been, are or may be used in the applications concerned. Their performance is discussed in terms of the theoretical models presented in earlier chapters. In addition, the principles of the application and the preparation of the materials are dealt with briefly. Appendices on some, often not-well-understood, issues follow (nomenclature, spectral units, literature, emission spectra).

We are very grateful to Mrs. Jessica Heilbrunn (Utrecht) who patiently typed the manuscript and did not complain too much when correction after correction appeared over many months. Miss Rita Bergt (München) was of help in drawing some of the figures. Some of our colleagues put original photographs at our disposal.

This book would not have been written without discussions with and inspiration from many colleagues over a long period of time. These contacts, some oral, some via written texts, cover a much wider range than the book itself. In the preparation of this book our communication with Drs. P.W. Atkins, F. Auzel, A. Bril, C.W.E. van Eijk, G.F. Imbusch, C.K. Jørgensen, and B. Smets has been very useful.

For many years we have enjoyed our work in the field of luminescence. We hope that this book will help the reader to understand luminescence phenomena, to design new and improved luminescent materials, and to find satisfaction in doing so.

Spring 1994

G. Blasse, Utrecht
B.C. Grabmaier, München

Table of Contents

Chapter 4 Nonradiative Transitions

Chapter 5 Energy Transfer

Chapter 6 Lamp Phosphors

Chapter 7 Cathode-Ray Phosphors

Chapter 8 X-Ray Phosphors and Scintillators (Integrating Techniques)

Chapter 9 X-Ray Phosphors and Scintillators (Counting Techniques)

Chapter 10 Other Applications

CHAPTER 1

A General Introduction to Luminescent Materials

This chapter addresses those readers for who luminescent materials are a new challenge. Of course you are familiar with luminescent materials: you meet them everyday in your laboratory and in your home. If this should come as a surprise, switch on your fluorescent lighting, relax in front of your television set, or take a look at the screen of your computer. Perhaps you would like something more specialized. Remember then your visit to the hospital for X-ray photography. Or the laser in your institute; the heart of this instrument consists of a luminescent material. However, such a high degree of specialization is not necessary. The packet of washing powder in your supermarket also contains luminescent material.

Now that we have been reminded of how full of luminescent materials our society is, the question arises "How do we define a luminescent material?" The answer is as follows: A luminescent material, also called a phosphor, is a solid which converts certain types of energy into electromagnetic radiation over and above thermal radiation. When you heat a solid to a temperature in excess of about 600°C, it emits (infra)red radiation. This is thermal radiation (and not luminescence). The electromagnetic radiation emitted by a luminescent material is usually in the visible range, but can also be in other spectral regions, such as the ultraviolet or infrared.

Luminescence can be excited by many types of energy. Photoluminescence is excited by electromagnetic (often ultraviolet) radiation, cathodoluminescence by a beam of energetic electrons, electroluminescence by an electric voltage, triboluminescence by mechanical energy (e.g. grinding), X-ray luminescence by X rays, chemiluminescence by the energy of a chemical reaction, and so on. Note that thermoluminescence does not refer to thermal excitation, but to stimulation of luminescence which was excited in a different way.

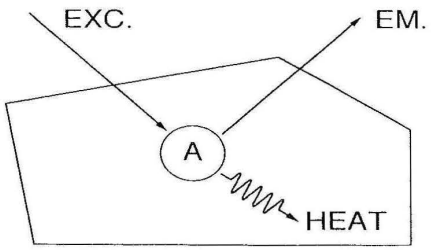

Fig. 1.1. A luminescent ion A in its host lattice. *EXC:* excitation; *EM:* emission (radiative return to the ground state); *HEAT:* nonradiative return to the ground state

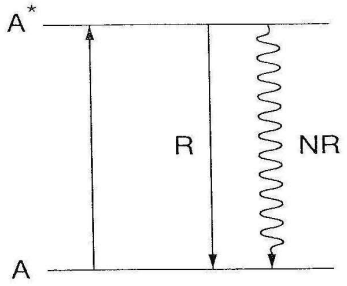

Fig. 1.2. Schematic energy level scheme of the luminescent ion A in Fig. 1.1. The *asterisk* indicates the excited state, *R* the radiative return and *NR* the nonradiative return to the ground state

In Fig. 1.1, we have drawn schematically a crystal or a grain of a photoluminescent material in order to illustrate the definition. Our system consists of a host lattice and a luminescent center, often called an activator. For example, consider the famous luminescent materials $Al_2O_3 : Cr^{3+}$ (ruby) and $Y_2O_3 : Eu^{3+}$. The host lattices are Al_2O_3 and Y_2O_3, the activators the Cr^{3+} and the Eu^{3+} ions.

The luminescence processes in such a system are as follows. The exciting radiation is absorbed by the activator, raising it to an excited state (Fig. 1.2). The excited state returns to the ground state by emission of radiation. This suggests that every ion and every material shows luminescence. This is not the case. The reason for this is that the radiative emission process has a competitor, viz. the nonradiative return to the ground state. In that process the energy of the excited state is used to excite the vibrations of the host lattice, i.e. to heat the host lattice. In order to create efficient luminescent materials it is necessary to suppress this nonradiative process.

The obvious characteristics to be measured on this system are the spectral energy distribution of the emission (the emission spectrum), and of the excitation (the excitation spectrum; which in this simple case is often equal to the absorption spectrum), and the ratio of the radiative and the nonradiative rates of return to the ground state. The latter determines the conversion efficiency of our luminescent material.

Let us for a second return to ruby ($Al_2O_3 : Cr^{3+}$). This is a beautiful red gemstone which shows a deepred luminescence under excitation with ultraviolet or visible radiation. Its spectroscopic properties were studied as early as 1867 by the famous scientist Becquerel, who used sunlight as the excitation source. He claimed that the color as well as the luminescence were intrinsic properties of the host lattice. This time, however, Becquerel was wrong. It is the Cr^{3+} ion which is responsible for the optical absorption of ruby in the visible and ultraviolet spectral regions. The host lattice Al_2O_3 does not participate at all in the optical processes. In fact Al_2O_3 is colorless. In the case of the ruby, the activator A in Fig. 1.1 is the Cr^{3+} ion and the host lattice is Al_2O_3. The host lattice of this luminescent material has no other function than to hold the Cr^{3+} ion tightly.

In many luminescent materials the situation is more complicated than depicted in Fig. 1.1, because the exciting radiation is not absorbed by the activator, but elsewhere. For example, we can add another ion to the host lattice. This ion may absorb

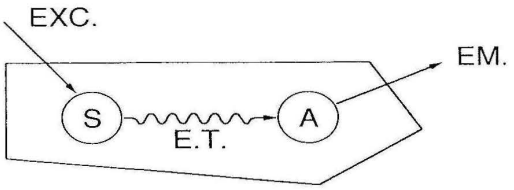

Fig. 1.3. Energy transfer from a sensitiser S to an activator A. Energy transfer is indicated by *E.T.* For further notation, see Fig. 1.1

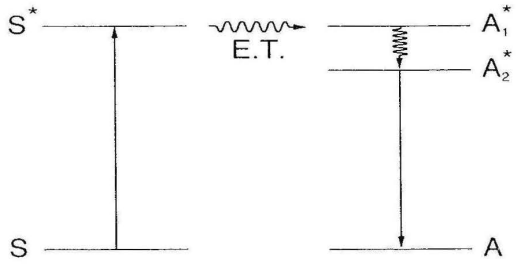

Fig. 1.4. Energy transfer from S to A. The S → S* transition is the absorption (or excitation), the $A_2^* \rightarrow A$ transition the emission. The level A_1^*, populated by energy transfer (*E.T.*), decays nonradiatively to the slightly lower A_2^* level. This prevents back transfer

the exciting radiation and subsequently transfer it to the activator. In this case the absorbing ion is called a sensitizer (see Fig. 1.3).

Another well-known example, viz. the lamp phosphor $Ca_5(PO_4)_3F : Sb^{3+}, Mn^{2+}$. Ultraviolet radiation is not absorbed by Mn^{2+}, but only by Sb^{3+}. Under ultraviolet irradiation, the emission consists partly of blue Sb^{3+} emission, and partly of yellow Mn^{2+} emission. Since the Mn^{2+} ion was not excited directly, the excitation energy was transferred from Sb^{3+} to Mn^{2+} (see Fig. 1.4). The luminescence processes can be written as follows, where $h\nu$ indicates radiation with frequency ν and the asterisk an excited state:

$$Sb^{3+} + h\nu \rightarrow (Sb^{3+})^*$$

$$(Sb^{3+})^* + Mn^{2}+ \rightarrow Sb^{3+} + (Mn^{2+})^*$$

$$(Mn^{2+})^* \rightarrow Mn^{2+} + h\nu.$$

These "equations" indicate absorption, energy transfer, and emission, respectively. If the Sb^{3+} ion has no Mn^{2+} ions in its vicinity, it gives its own blue emission. For those of you who are not familiar with solids, please realize that in general the concentrations of the luminescent centers are of the order of a 1 mol.%, and that the centers are, in first approximation, distributed at random over the host lattice.

Sometimes, however, the activator concentration can be 100%. This illustrates the rather complicated nature of luminescent materials. Actually these high activator concentrations which occur in some cases were not understood for a long time, preventing

progress in our understanding of luminescent materials. A famous example of such a high-concentration material is $CaWO_4$ where the tungstate group is the luminescent center. Simultaneously it is a building unit of the host lattice which consists of Ca^{2+} and WO_4^{2-} ions. This material was used for 75 years in X-ray photography, and in tungsten mines its luminescence is used to find $CaWO_4$. The miners use ultraviolet lamps to find the tungstate-rich ores by their visible luminescence! Chapter 5 discusses why a high concentration of activators is sometimes fatal for luminescence, whereas in other cases such high concentrations yield very high luminescence outputs.

In stead of exciting a low concentration of sensitizers or activators, we can also excite the host lattice. This is, for example, what happens if we excite with X rays or electron beams. In many cases the host lattice transfers its excitation energy to the activator, so that the host lattice acts as the sensitizer. Again a few examples. In $YVO_4 : Eu^{3+}$ ultraviolet radiation excites the vanadate groups, i.e. the host lattice. The emission, however, consists of Eu^{3+} emission. This shows that the host lattice is able to transfer its excitation energy to the Eu^{3+} ions. Another example is $ZnS : Ag^+$, the blue-emitting cathode-ray phosphor used in television tubes. Ultraviolet radiation, electron beams and X rays excite the sulfide host lattice which transfers this excitation energy rapidly to the activators (the Ag^+ ions).

In spite of the fact that we did not discuss any fundamental background (this will be done in Chapters 2-5), you have met by now the more important physical processes which play a role in a luminescent material:

- absorption (excitation) which may take place in the activator itself, in another ion (the sensitizer), or in the host lattice (Chapter 2)
- emission from the activator (Chapter 3)
- nonradiative return to the ground state, a process which reduces the luminescence efficiency of the material (Chapter 4)
- energy transfer between luminescent centers (Chapter 5).

After this short, general introduction into the operation of a luminescent material, we now turn to a similar introduction to the applications of luminescent materials.

Photoluminescence is used in fluorescent lamps. This application was even used before the Second World War. The lamp consists of a glass tube in which a low-pressure mercury discharge generates ultraviolet radiation (85% of this radiation consists of 254 nm radiation). The lamp phosphor (or a mixture of lamp phosphors) is applied to the inner side of the tube. This phosphor converts the ultraviolet radiation into white light. The efficiency of conversion of electricity to light is in a fluorescent lamp considerably higher than in an incandescent lamp.

The introduction of rare-earth activated phosphors in fluorescent lamps during the last decade has improved the light output and the colour rendering drastically. As a consequence this type of lighting is no longer restricted to shops and offices, but is now also suitable for living rooms. It is interesting to note that in this way chemical elements which for a long time have been considered as rare, peculiar, and hard to separate, have penetrated our houses. A modern fluorescent lamp contains the following rare earth ions: divalent europium, trivalent cerium, gadolinium, terbium, yttrium and europium. You will find more about this important application of photoluminescence in Chapter 6.

One can hardly imagine life today without cathode-ray tubes. Think of your television set or your computer screen. In a cathode-ray tube the luminescent material is applied on the inner side of the glass tube and bombarded with fast electrons from the electron gun in the rear end of the tube. When the electron hits the luminescent material, it emits visible light. In the case of a colour television tube there are three electron guns, one irradiating a blue-emitting luminescent material, so that it creates a blue pictures, whereas two others create in a similar way a green and a red picture.

One fast electron creates in the luminescent material many electron-hole pairs which recombine on the luminescent center. This multiplication is one of the factors which have determined the success of the cathode-ray tube as a display. It will be clear that the luminescent materials applied belong to the class of materials where excitation occurs in the host lattice. They will be discussed in Chapter 7 where we will also deal with materials for projection television. In this way the display screen can have a diameter of 2 m. This application puts requirements on luminescent materials which are hard to satisfy.

Let us now turn to materials which are able to convert X-ray irradiation into visible light. Röntgen discovered X rays in 1895, and realized almost immediately that this type of radiation is not very efficient at exposing photographic film, because the film does not absorb the X rays effectively. As a consequence long irradiation times are required. Nowadays we know that this is bad for the patient. There is also a practical objection against long irradiation times: the patient is a moving object (he breathes and may, in addition, make other movements), so that sharp pictures can only be obtained if the irradiation time is short.

Therefore Röntgen initiated a search for luminescent materials which absorb X rays efficiently and convert their energy into radiation which is able to blacken the photographic film. Soon it was found that $CaWO_4$ with a density of 6.06 $g.cm^{-3}$ was able to do so. This compound was used for a very long time in the so-called X-ray intensifying screens. A schematic picture of X-ray photography with this method is given in Fig. 1.5.

Just as in the field of lamp phosphors and (partly) cathode-ray phosphors, $CaWO_4$ lost its leading position to rare-earth activated X-ray phosphors (see chapter 8). As a salute to this old champion, but also for your information, we give in Fig. 1.6 the crystal structure of $CaWO_4$ which illustrates the build-up of the lattice from Ca^{2+} ions and luminescent WO_4^{2-} groups, and in Fig. 1.7. an electron micrograph of a commercial $CaWO_4$ powder.

A recent development in this field is the introduction of storage phosphors. These materials have a "memory" for the amount of X rays which has been absorbed at a given spot of the screen. By scanning the irradiated screen with an (infra)red laser, visible luminescence is stimulated. Its intensity is proportional to the amount of X rays absorbed. Chapter 8 discusses how to produce such materials and the physics behind these phenomena.

As an example of a more specialized character, we should mention the case of X-ray computed tomography. This method of medical radiology generates cross-sectional images of the interior of the human body (see Fig. 1.8). Besides the X-ray source, the key component is the detector consisting of about 1000 pieces of a luminescent solid (crystals or ceramics) which are connected to photodiodes or -multipliers. The

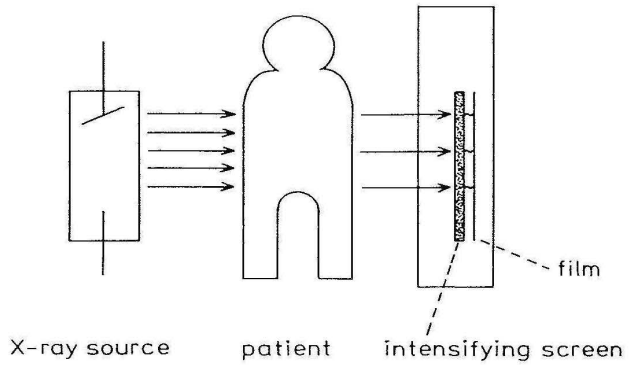

Fig. 1.5. Schematic representation of a medical radiography system based on the use of an intensifying screen

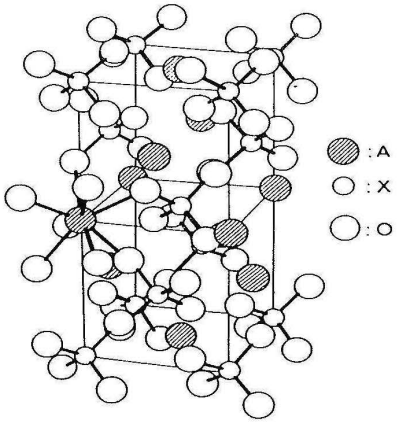

Fig. 1.6. Crystal structure of $CaWO_4$ (scheelite). The general formula is AXO_4 where *A* are the larger and *X* the smaller metal ions

luminescent material has to show sharply defined properties in order to be acceptable for this application.

After these examples of X-ray photography, you will not be surprised to learn that α and γ radiation can also be detected by luminescent materials, which, in this case, are usually called scintillators and are often in the form of large single crystals. The applications range from medical diagnostics (for example positron emission tomog-

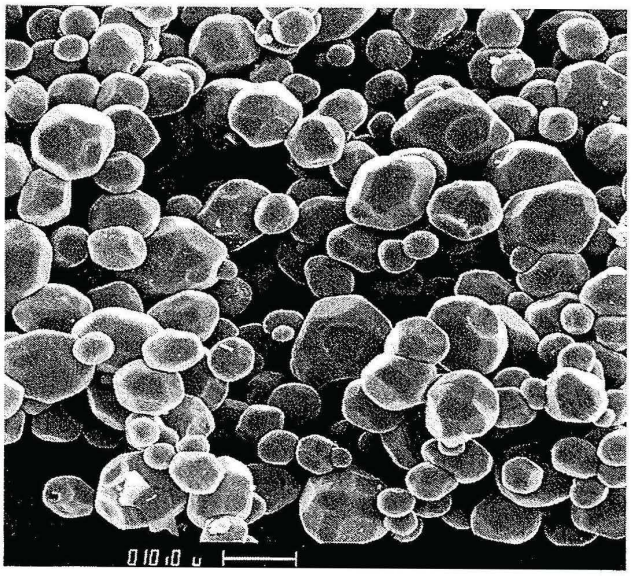

Fig. 1.7. $CaWO_4$ powder phosphor (1000×)

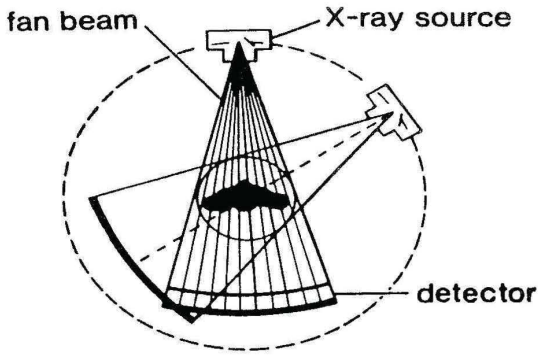

Fig. 1.8. The principle of X-ray computed tomography. The patient is in the center of the picture. Source and detector rotate around the patient

raphy (PET)) to nuclear and high-energy physics. A spectacular application in the latter field is the use of 12 000 crystals of $Bi_4Ge_3O_{12}$ ($3 \times 3 \times 24$ cm^3) as a detector for electrons and photons in the LEP machine at CERN (Geneva). Scintillators will be discussed in Chapter 9.

As a matter of fact there are many other types of application. Some of these are discussed in Chapter 10. Before you get the impression that (the application of)

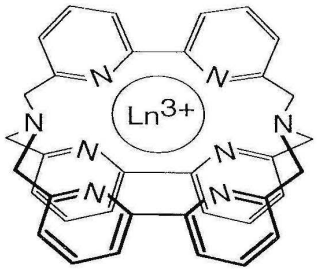

Fig. 1.9. The $[Ln \subset bpy.bpy.bpy]^{3+}$ cryptate

luminescence is restricted to solids, we should pick out one of these, viz. fluoro-immunoassay, which is based on luminescent molecules. This is a method used in immunology in order to detect biomolecules. The method is superior to other methods (such as those using radioactive molecules) as far as sensitivity and specificity are concerned. It is used particularly in the clinical investigation of compounds in low concentration and consists of the labelling of samples with luminescent species and the measurement of their luminescence.

One of the molecules which plays a role in this field is depicted in Fig. 1.9. The luminescent species is the Eu^{3+} ion which we met already above. It is surrounded by a cage containing molecules of bipyridine. The whole complex is called a cryptate and its formula is written as $[Eu \subset bpy.bpy.bpy]^{3+}$. The cage protects the Eu^{3+} ion against the (aqueous) surroundings which tries to quench the luminescence. If this cryptate is excited with ultraviolet radiation, the bipyridine molecules absorb the exciting radiation and transfer their excitation energy subsequently to the Eu^{3+} ion which then shows its red luminescence.

Coordination chemists call this transfer from bipyridine to Eu^{3+} an antenna effect. It is of course exactly the same phenomenon which we described above (Fig. 1.3). In solid state research the effect is simply called energy transfer. In Chapter 10 we will see that the physics of molecules like cryptates is very similar to that of solids like those depicted in Fig. 1.3.

Finally that intriguing application yielding the laser. In luminescence the radiative decay of the excited state to the ground state occurs by spontaneous emission, i.e. the emission processes on different activator ions are not correlated. If, by some means, the majority of the luminescent ions are in the excited state (this situation is called population inversion), a single spontaneously emitted photon (quantum of radiation) may stimulate other excited ions to emit. This process is called stimulated emission. It is monochromatic, coherent and non-divergent. Laser action depends on emission by a stimulated process. Actually the word laser is an acronym for light amplification by stimulated emission of radiation. This book does not deal with lasers or laser physics. However, we will deal with the material where the stimulated emission is generated if this is useful for our purpose. Every laser material is after all also a luminescent material.

If you are surprised, remember the gemstone ruby ($Al_2O_3 : Cr^{3+}$) mentioned in the beginning of this chapter. Becquerel started long ago to study its luminescence and spectroscopy. Ruby was and is the start of several interesting phenomena in solid state physics. Probably the most important of these is the first solid state laser which was based on ruby (Maiman, 1960). This illustrates the connection between luminescence and lasers. On the other hand, in more recent years it has only been possible to unravel and understand luminescence processes by using laser spectroscopy.

This introductory chapter should have stimulated or excited you to read on and to become acquainted with the physics and the chemistry of luminescence and luminescent materials.

References

Chapter 1 does not have specific literature references in view of its general and introductory character. Those who are invited by this chapter to improve their knowledge of the basic physics and chemistry of energy levels, ions, spectroscopy and/or solid state chemistry, are referred to general textbooks in the field of physical and inorganic chemistry. Our personal preferences are the following: P.W. Atkins (1990) Physical Chemistry, 4th edn, Oxford University Press; and D.F. Shriver, P.W. Atkins and C.H. Langford (1990) Inorganic Chemistry, Oxford University Press (chapters 14 and 18). The ruby history has been reviewed by G.F. Imbusch (1988) In: W.M. Yen and M.D. Levenson (eds) Lasers, Spectroscopy and New Ideas. Springer Berlin Heidelberg New York. Those who want to judge the great progress in luminescent materials during the last few decades should compare this book with the review paper by J.L. Ouweltjes, Luminescence and Phosphors, Modern Materials 5 (1965) p. 161.

CHAPTER 2

How Does a Luminescent Material Absorb Its Excitation Energy?

2.1 General Considerations

A luminescent material will only emit radiation when the excitation energy is absorbed. These absorption processes will be the subject of this chapter with stress on excitation with ultraviolet radiation. The emission process will be treated in the next chapter.

Let us consider an optical absorption spectrum of a well-known luminescent material, viz. $Y_2O_3 : Eu^{3+}$. Figure 2.1 presents this spectrum in a schematic form. Starting on the long wavelength (i.e. low energy) side, the following features can be noted:

- very weak narrow lines
- a broad band with a maximum at 250 nm
- a very strong absorption region for $\lambda \leq 230$ nm.

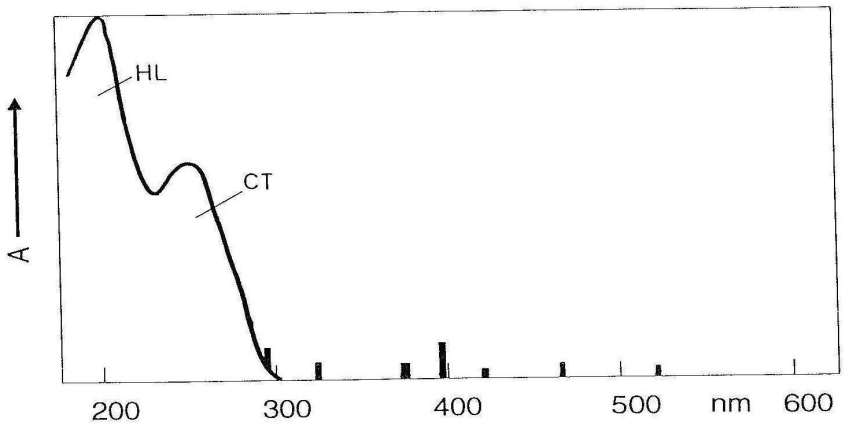

Fig. 2.1. Schematic representation of the absorption spectrum of $Y_2O_3 : Eu^{3+}$. The value of A gives the absorption strength in arbitrary units. The narrow lines are transitions within the $4f^6$ configuration of Eu^{3+}, CT is the Eu^{3+}-O^{2-} charge-transfer transition, and HL the host lattice (Y_2O_3) absorption

The absorption spectrum of pure Y_2O_3 shows only the latter absorption. Therefore the lines and the 250 nm band must be due to Eu^{3+}, and the absorption at $\lambda < 230$ nm to the host lattice Y_2O_3.

Let us now consider the excitation spectrum of the Eu^{3+} emission of $Y_2O_3 : Eu^{3+}$. Such a spectrum yields the luminescence output as a function of the exciting wavelength, so that there should be a correlation with the absorption spectrum. The excitation spectrum of $Y_2O_3 : Eu^{3+}$ shows a striking agreement with the absorption spectrum of $Y_2O_3 : Eu^{3+}$. This means the following:

- if the Eu^{3+} ions are excited directly (sharp lines, 250 nm band), luminescence from Eu^{3+} is observed. Less trivial is the second observation:
- if the host lattice Y_2O_3 is excited ($\lambda \leq 230$ nm), luminescence from Eu^{3+} is observed. Consequently, the excitation energy absorbed by the host lattice Y_2O_3 is transferred to the activator Eu^{3+}. These transfer processes will be considered later in detail (Chapter 5). For the moment it is important to realize that absorption of excitation energy is not restricted to the activator itself, but can also occur elsewhere.

High-energy excitation always excites the host lattice. Examples are fast electrons, γ rays, X rays. Direct excitation of the activator is only possible with ultraviolet and/or visible radiation. The phosphor $Y_2O_3 : Eu^{3+}$, for example, is excited in the activator itself (the 250 nm band) when applied in a luminescent lamp (254 nm excitation), but in the host lattice when applied as a cathode-ray or X-ray phosphor.

In this chapter we are dealing mainly with absorption of ultraviolet or visible radiation, because its wavelength can be easily varied and this indicates exactly what and where we are exciting. As H.A. Klasens, a pioneer in luminescent materials, used to say: ultraviolet excitation compares to striking one key of the piano, cathode-ray or X-ray excitation compares to throwing the piano down the stairs.

Let us now return to the absorption spectrum of Figure 2.1. A central problem of absorption spectra can immediately be noted, viz. why are certain spectral features so narrow and others so broad, and why have some such a low and others such a high intensity. To these questions we will give an answer in a simplified form. Detailed presentations can be found in many books [1-3].

The shape of an optical absorption band, i.e. narrow or broad, can be explained using the configurational coordinate diagram. Such a diagram shows the potential energy curves of the absorbing center as a function of a configurational coordinate. This coordinate describes one of the vibrational modes of the centre involved. We will follow the method of many textbooks in considering the vibrational mode in which the central metal ion is at rest and the surrounding ligands are moving in phase away from the metal ion and coming back. This is the so-called symmetrical stretching (or breathing) mode. Figure 2.2 gives a schematic example.

The configurational coordinate diagram for this mode reduces to a plot of the energy E versus the metal-ligand distance R, since R is the structural parameter which varies during the vibration. In doing so, the reader should realize that we neglect all other vibrational modes. In older textbooks this was considered to be a justified approximation, but later it was shown to be a dangerous one, because it neglects distortions in the excited state. These often occur, as we will see later in this book.

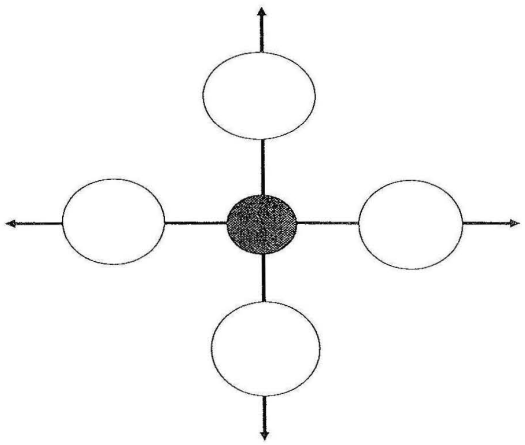

Fig. 2.2. Symmetrical stretching vibration of a square-planar complex. The ligands (open circles) move in phase from and to the central metal ion

Figure 2.3. shows a configurational coordinate diagram where E is plotted versus R. Consider first the curve for the lowest state, the ground state. Its shape is parabolic with a minimum at R_0. This parabolic shape follows from the fact that the vibrational motion is assumed to be harmonic, i.e. the restoring force F is proportional to the displacement: $F = -k(R - R_0)$. A force of this form corresponds to a potential energy whose dependence on R is parabolic: $E = \frac{1}{2}k(R - R_0)^2$. The minimum R_0 of the parabola corresponds to the equilibrium distance in the ground state.

The quantum mechanical solution of this problem (known as the harmonic oscillator) yields for the energy levels of the oscillator $E_v = (v + \frac{1}{2})h\nu$, where $v = 0, 1, 2, \ldots$. and ν is the frequency of the oscillator. Part of these levels have been drawn in Figure 2.3. For a simple derivation, see e.g. Ref. [4].

The wave functions of these vibrational levels are also known. For our purpose the more important information is that in the lowest vibrational level ($v = 0$) the highest probability of finding the system is at R_0, whereas for high values of v it is at the turning points, i.e at the edges of the parabola (like in the classic pendulum) (see Figure 2.4.).

What has been said about the ground state holds also for the excited states: in the E-R diagram they occur also as parabolas, but with different values of the equilibrium distance (R_0') and force constant (k'). These differences are due to the fact that in the excited state the chemical bond is different from that in the ground state (often weaker). This is also shown in Figure 2.3, where the parabolas are shifted relative to each other over a value ΔR.

Before considering optical absorption processes in the configurational coordinate model, we would like to draw attention to the fact that what we have done is consider the interaction between the absorbing metal ion and the vibrations of its surroundings. Transitions between two parabolas are electronic transitions. Our model enables us, in principle, to consider the interaction between the electrons and the vibrations of the

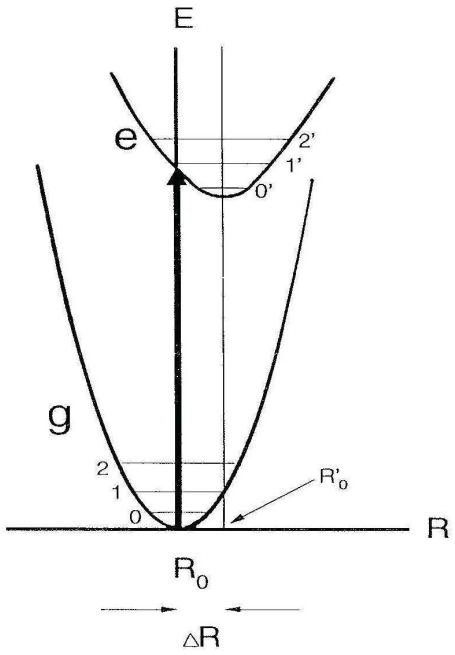

Fig. 2.3. Configurational coordinate diagram (see also text). The ground state (g) has the equilibrium distance R_0; the vibrational states $v = 0, 1, 2$ are shown. The excited state (e) has the equilibrium distance R_0'; the vibrational states $v' = 0, 1, 2$ are shown. The parabola offset is $\Delta R (= R_0' - R_0)$

optical centre under consideration. Actually the value of $\Delta R = R_0' - R_0$ is a qualitative measure of this interaction.

In optical absorption the centre is promoted from its ground state to an excited state. How is such a transition described in the configurational coordinate diagram of Figure 2.3? It is important to realize that optical transitions occur in this diagram as vertical transitions. The reason for this is that a transition from the ground state to the excited state is electronic, whereas horizontal displacements in this diagram are nuclear, the distance R being an internuclear distance. Since the electrons move much faster than the nuclei, the electronic transition takes, in good approximation, place in static surroundings. This implies a vertical transition in Figure 2.3. The nuclei take their appropriate positions only later (next chapter).

The optical absorption transition starts from the lowest vibrational level, i.e. $v = 0$. Therefore, the most probable transition occurs at R_0 where the vibrational wave function has its maximum value (see Figure 2.5). The transition will end on the edge of the excited state parabola, since it is there that the vibrational levels of the excited state have their highest amplitude. This transition corresponds to the maximum of the absorption band. It is also possible, although less probable, to start at R values larger or smaller than R_0. This leads to the width of the absorption band (Figure 2.5), because for $R > R_0$ the energy difference of the transition will be less than for $R = R_0$, and for $R < R_0$ it will be larger.

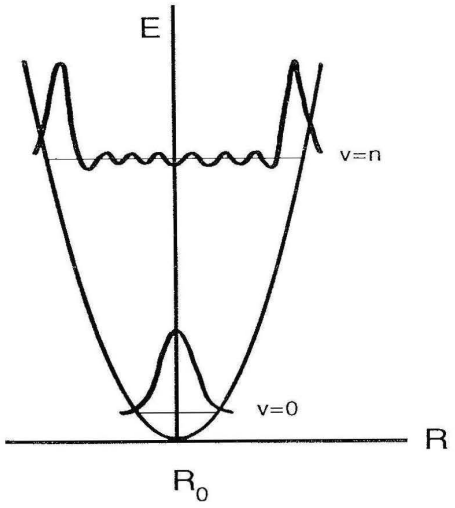

Fig. 2.4. The vibrational wave functions for the lowest vibrational level (v = 0) and a high vibrational level (v = n)

If $\Delta R = 0$, the two parabolas lie exactly above each other and the band width of the optical transition vanishes: the absorption band becomes a narrow line.

It can be simply shown [1,4] that the probability for an optical transition between the $v = 0$ vibrational level of the ground state and the $v = v'$ vibrational level of the excited state is proportional to

$$\langle e|r|g\rangle \langle \chi_{v'}|\chi_o\rangle . \tag{2.1}$$

Here the functions e and g present the electronic wave functions of the excited state and the ground state, respectively; r is the electric-dipole operator driving the transition; and χ are the vibrational wave functions. In order to consider the whole absorption band, one has to sum over v'.

The first part of eq. (2.1) is the electronic matrix element, which is independent of the vibrations. The second part gives the vibrational overlap. The former gives the intensity of the transition as will be shown below, the latter determines the shape of the absorption band.

The latter statement can be illustrated as follows. When $\Delta R = 0$, the vibrational overlap will be maximal for the levels $v = 0$ and $v' = 0$, since the vibrational wave functions involved have their maxima at the same value of R, viz. R_o. The absorption spectrum consists of one line, corresponding to the transition from $v = 0$ to $v' = 0$. This transition is called the zero-vibrational or no-phonon transition, since no vibrations are involved. If, however, $\Delta R \neq 0$, the $v = 0$ level will have the

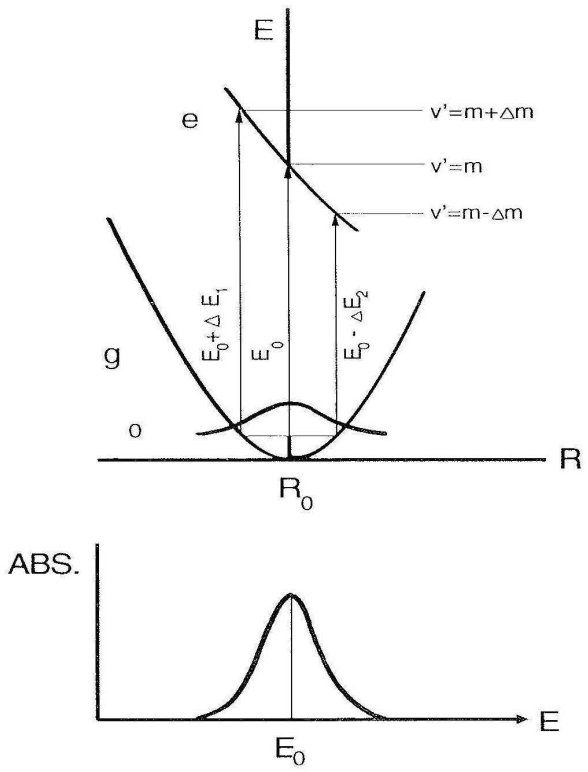

Fig. 2.5. The optical absorption transition between two parabolas which have an offset relative to each other in the configurational coordinate diagram consists of a broad absorption band. See also text

maximal vibrational overlap with several levels $v' > 0$, and a broad absorption band is observed.

The broader the absorption band, the larger the value of ΔR. The width of an absorption band informs us immediately how large the difference in ΔR (and how large the difference in chemical bonding) between the excited state and the ground state is.

It is usual to call the $\Delta R = 0$ situation the weak-coupling scheme, $\Delta R > 0$ the intermediate-coupling scheme, and $\Delta R \gg 0$ the strong-coupling scheme. The word coupling relates to the coupling between the electrons and the vibrations of the center considered. The value of ΔR measures the strength of this interaction.

At higher temperature, the initial state may also be one with $v > 0$. This results in band broadening. This well-known phenomenon is easily explained by the configurational coordinate diagram.

Now we return to the intensity of the optical absorption transition which is contained in the matrix element $\langle e|r|g\rangle$. Not every possible transition between g and e does occur as an optical transition, since these are gouverned by selection rules.

Here we should mention two important selection rules, viz.

- the spin selection rule which forbids electronic transitions between levels with different spin states ($\Delta S \neq 0$)
- the parity selection rule which forbids electronic (electric-dipole) transitions between levels with the same parity; examples are electronic transitions within the $d$shell, within the $f$shell, and between the $d$and the s shells.

In solids, the selection rules can seldom be considered as absolute rules. The situation is reminiscent of towns with low traffic morals: when the traffic light is green everyone crosses (allowed transition, no selection rules), at red there are still a few people who cross against the rules (forbidden transition, but selection rule slightly relaxed). The relaxation of selection rules is connected to wavefunction admixtures into the original, unperturbed wave functions. This can be due to several physical phenomena, like spin-orbit coupling, electron-vibration coupling, uneven crystal-field terms, etc. Their treatment lies outside the scope of this book. The reader is referred to Refs. [1] and [3].

Let us now return to Figure 2.1. The host lattice absorption band of Y_2O_3 is very broad and intense. This means that the excited state is strongly different from the ground state. Actually the highest occupied levels of the ground state are the $2p$ orbitals of oxygen; the lowest unoccupied levels of the excited state are a mixture of $3s$ orbitals of oxygen and $4d$of yttrium. Without going into detail, the reader will understand that the lowest optical transition in Y_2O_3 results in large changes in chemical bonding and ΔR.

The Eu^{3+} absorption features have lower intensity. This is in the first place due to its lower concentration (there is about 1% Eu in the sample for which the spectrum of Figure 2.1 is measured). The 250 nm absorption band is a charge-transfer transition in the Eu^{3+}–O^{2-} bond: an electron jumps from oxygen to europium. Consequently ΔR is large and the absorption band broad. There is no selection rule which reduces the intensity. The narrow weak lines are due to electronic transitions within the non-bonding $4f^6$ shell of Eu^{3+}. As a consequence $\Delta R = 0$, yielding narrow lines. The parity-selection rule forbids these transitions, and they are very weak indeed (often more than 10^6 times weaker than allowed transitions).

This paragraph dealt with the properties of absorption bands in the ultraviolet and visible region in general. Section 2.3 deals with specific cases.

2.2 The Influence of the Host Lattice

If we consider a given luminescent centre in different host lattices, the optical properties of this center are usually also different. This is not so surprising, since we change the direct surroundings of the luminescent center. In this paragraph some of these

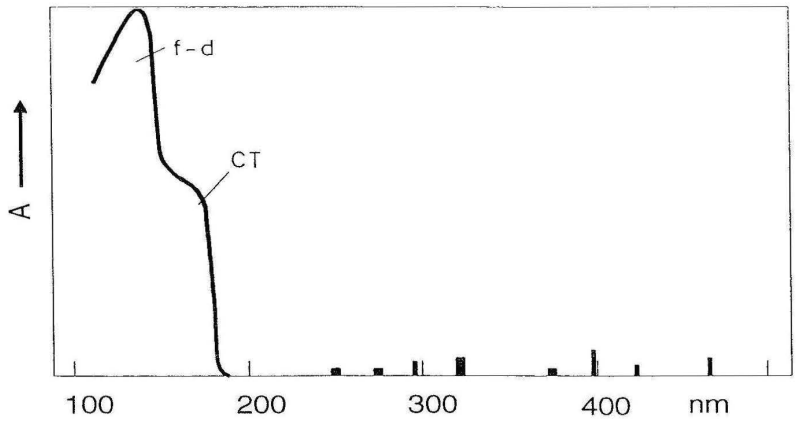

Fig. 2.6. Schematic representation of the absorption spectrum of $YF_3 : Eu^{3+}$. The indications CT and $f \rightarrow d$ relate to the Eu^{3+}–F^- charge-transfer and the $Eu^{3+} 4f^6 \rightarrow 4f^5 5d$ transitions, respectively

effects will be considered. They are of prime importance in the materials science of luminescent materials: if we would understand how the luminescence properties of an optical center depend on the host lattice, it would be easy to predict all the luminescent materials.

To illustrate the influence of the host lattice on the optical absorption of a center, we consider the absorption spectrum of $YF_3 : Eu^{3+}$ (Fig. 2.6), and compare it with that of $Y_2O_3 : Eu^{3+}$ (Fig. 2.1). The following differences are immediately obvious.

- the host lattice absorption band of Y_2O_3 has disappeared. That of YF_3 is not observed; it is situated at even shorter wavelengths than given in Figure 2.6.
- the charge-transfer absorption band of $Y_2O_3 : Eu^{3+}$ has disappeared. In $YF_3 : Eu^{3+}$ it appears at about 150 nm. This shows that it takes much more energy to remove an electron from an F- ion than from an O^{2-} ion.
- in addition the absorption spectrum of $YF_3 : Eu^{3+}$ shows the allowed $4f \rightarrow 5d$ transitions of Eu^{3+} at about 140 nm.
- in both absorption spectra the transitions within the $4f^6$ configuration of Eu^{3+} are observed as sharp and weak lines. Since the $4f$electrons are well shielded from the surroundings by completely filled $5s$ and $5p$ orbitals, the influence of the surroundings of the Eu^{3+} ion is expected to be small indeed.

Careful inspection of these narrow absorption lines shows clear differences which cannot be seen in the rough Figs. 2.1 and 2.6. In the fluoride they are even less intense than in the oxide, in the fluoride their spectral positions tend to be at slightly higher energy than in the oxide, and their splitting pattern under high resolving power is different in the two compositions.

Let us now consider the main factors responsible for different spectral properties of a given ion in different host lattices. The first factor to be mentioned is covalency [5-8]. For increasing covalency the interaction between the electrons is reduced, since they spread out over wider orbitals. Consequently, electronic transitions between energy

Table 2.1. The nephelauxetic effect for Bi^{3+} and Gd^{3+}. Covalency increases from top to bottom.

Bi^{3+} [9]		Gd^{3+} [10]	
Host lattice	$^1S_0$ - $^3P_1$ (cm^{-1})*	Host Lattice	$^8S \rightarrow {}^6P_{7/2}$ (cm^{-1})**
YPO_4	43.000	LaF_3	32.196
YBO_3	38.500	$LaCl_3$	32.120
$ScBO_3$	35.100	$LaBr_3$	32.096
La_2O_3	32.500	$Gd_3Ga_5O_{12}$	31.925
Y_2O_3	30.100	$GdA1O_3$	31.923

* lowest component of the $6s^2 \rightarrow 6s6p$ transition
** lowest transitions within the $4f^7$ shell

Table 2.2. The maximum of the Eu^{3+} charge-transfer transition in several host lattices [9].

Host lattice	Maximum Eu^{3+} CT (10^3 cm^{-1})
YPO_4	45
YOF	43
Y_2O_3	41.7
$LaPO_4$	37
La_2O_3	33.7
LaOCl	33.3
Y_2O_2S	30

levels with an energy difference which is determined by electron interaction shift to lower energy for increasing covalency. This is known as the nephelauxetic effect[1]. Table 2.1 gives two examples of a different nature, viz. for Bi^{3+} ($6s^2$) and for Gd^{3+} ($4f^7$). The former has a $6s^2 \rightarrow 6s6p$ absorption transition. The $6s$ and $6p$ electrons reside on the surface of the ion and the nephelauxetic effect is large. The latter has a weak absorption due to a transition within the $4f^7$ shell. This lies inside the ion, and the nephelauxetic effect is very small. In the same way the slightly higher positions of the transitions within the $4f^6$ shell of the Eu^{3+} ion in YF_3 compared to Y_2O_3 (see above) are also an illustration of this nephelauxetic effect.

Higher covalency means also that the electronegativity difference between the constituting ions becomes less, so that charge-transfer transitions between these ions shift to lower energy. This was mentioned already above, where the charge-transfer absorption band of Eu^{3+} in the fluoride YF_3 was observed to be at higher energy than in the more covalent oxide Y_2O_3. Table 2.2 gives some more examples. In sulfides europium is usually divalent [11], since the charge-transfer state of Eu^{3+} in sulfides lies at such low energy that the trivalent state is no longer stable.

Similar observations have been made for other ions with charge transfer transitions [5-7].

1 The word nephelauxetic means (electron)cloud expanding.

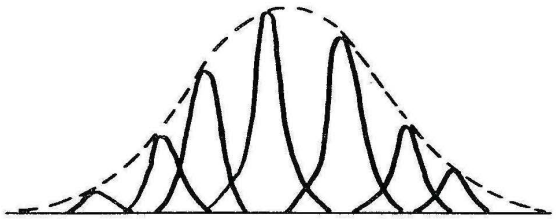

Fig. 2.7. Inhomogeneous broadening. The individual absorption transitions vary slightly from site to site in the host lattice. The broken line indicates the experimentally observed absorption spectrum

Another factor responsible for the influence of the host lattice on the optical properties of a given ion is the crystal field. This is the electric field at the site of the ion under consideration due to the surroundings. The spectral position of certain optical transitions is determined by the strength of the crystal field, the transition metal ions being the most well-known and clear example. For example, why is Cr_2O_3 green, but $Al_2O_3 : Cr^{3+}$ red, whereas both compositions have the same crystal structure? The qualitative answer is simple: in ruby ($Al_2O_3 : Cr^{3+}$) the Cr^{3+} ions (which are responsible for the color) occupy the smaller Al^{3+} sites, so that they feel a stronger crystal field than in Cr_2O_3. Therefore the optical transitions in ruby are at higher energy than in Cr_2O_3, so that the color of the two compositions is different.

In addition the crystal field is responsible for the splitting of certain optical transitions. Obvious is the following statement: different host lattices → different crystal fields → different splittings. In this way the optical center can serve as a probe of the surroundings: observed splittings yield the symmetry of the site.

Crystal fields of uneven (ungerade) symmetry are able to lift the parity selection rule. The reader should not underestimate the importance of such a, seemingly-academic, statement: there would be no color television, and no energy-saving luminescent lamps without uneven-symmetry crystal fields, as we will see later.

Up till now, it has been tacitly assumed that the surroundings and the symmetry of each center in the solid are the same. This is the case for Eu^{3+} in YF_3, the crystallographic sites of all Y^{3+} ions being equal. It should be realized that, in powders, the external, and also the internal surface may be large, and that Eu^{3+} ions near this surface experience a covalency and a crystal field which differs from the bulk. These Eu^{3+} ions have their optical transitions at energies which are slightly different from those in the bulk. Therefore the features in the spectra broaden. This is called inhomogeneous broadening (see Fig. 2.7). Point defects in the crystal structure yield also a contribution to this broadening.

The simple-looking $Y_2O_3 : Eu^{3+}$ is already more complicated, since the crystal structure offers for Y^{3+} two crystallographic sites with different symmetry. The Eu^{3+} ions are found on both sites with different spectral properties.

Pronounced inhomogeneous broadening occurs in glasses where all optical centers differ from site to site due to the absence of translational symmetry. Absorption bands in glasses are, therefore, always broader than in crystalline solids.

2.3 The Energy Level Diagrams of Individual Ions

In this section some specific (groups of) ions will be discussed more in detail as far as necessary for an understanding of the luminescence of luminescent materials. For more details the reader is referred to other books (for example, Refs [1,7,8]). For simplicity the energy level diagrams will be presented for one distance, viz. the equilibrium distance of the ground state. Therefore they contain less information than a configurational coordinate diagram (like those in Figs 2.3 and 2.5).

2.3.1 The Transition Metal Ions (d^n).

Transition metal ions have an incompletely filled $d$shell, i.e. their electron configuration is $d^n (0 < n < 10)$. The energy levels originating from such a configuration have been calculated by Tanabe and Sugano taking the mutual interaction between the $d$electrons as well as the crystal field into account. Figures 2.8–2.10 give, as an example, the results for the configurations d^1, d^3 and d^5.

On the utmost left-hand side (crystal field $\Delta = 0$) we find the energy levels of the free ion. Many of these levels split into two or more levels for $\Delta \neq 0$, as for example in a solid. The lowest level, i.e. the ground state, coincides with the x-axis. For the free ion the levels are marked ^{2S+1}L, where S presents the total spin quantum number, and L the total orbital angular momentum. Values of L may be 0 (indicated by S), 1 (P), 2 (D), 3 (F), 4 (G), etc. The degeneracy of these levels is 2L+1 and may be lifted by the crystal field. Crystal-field levels are marked ^{2S+1}X, where X may be A (no degeneracy), E (twofold degeneracy) and T (threefold degeneracy). Subscripts indicate certain symmetry properties. For more details the reader is referred to Refs [12] and [13]. The indicated nomenclature can be checked in Figs 2.8–2.10.

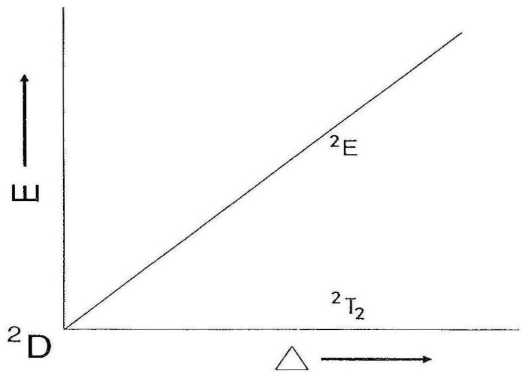

Fig. 2.8. The energy levels of the d^1 configuration as a function of the octahedral crystal field Δ. The free ion level is ^{2}D

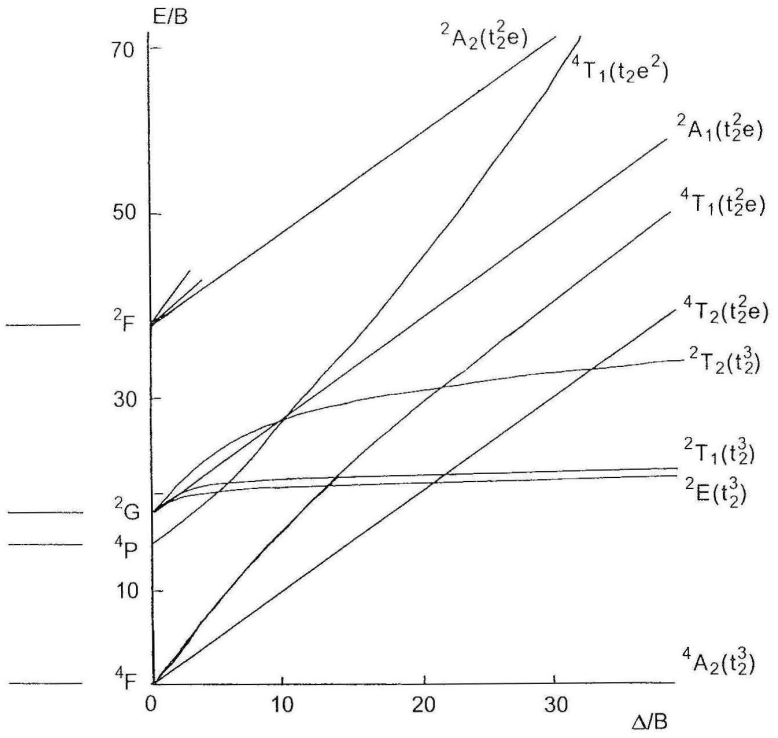

Fig. 2.9. Tanabe-Sugano diagram for the d^3 configuration. Free-ion levels on the left-hand side; crystal-field levels (with occupation of the one-electron crystal-field levels in parentheses) on the right-hand side. Note that levels belonging to the same subconfiguration tend to run parallel. The energy E and the octahedral crystal field Δ are plotted relative to B, an interelectronic repulsion parameter

Figure 2.8 (d^1 configuration) is the simplest of these three figures. The free ion has fivefold orbital degeneracy (^{2}D) which is split into two levels (^{2}E and $^2T_2$) in octahedral symmetry. In the figures the crystal field is taken octahedral, since octahedral coordination is quite common for transition metal ions. The only possible optical absorption transition is from $^2T_2$ to ^{2}E. This is shown in Fig. 2.11. The energy difference $^2E - {}^2T_2$ is equal to Δ, the crystal field strength. For trivalent transition metal ions Δ is about 20 000 cm^{-1}, i.e. the corresponding optical transition is situated in the visible spectral region. This explains why transition metal ions are usually nicely colored. The $^2T_2 \rightarrow {}^2$E transition is a clear example of a transition the energy of which is determined by the strength of the crystal field.

Note, however, that this transition is a forbidden one, since it occurs between levels of the d shell. Therefore the parity does not change. Actually the color of transition metal ions is never intense, as far as this type of transitions, also called crystal-field transitions, are involved. The parity selection rule is relaxed by coupling of the electronic transition with vibrations of suitable symmetry [13]. In tetrahedral symmetry, however, the centre of symmetry is lacking, and the parity selection rule is also relaxed in another way, viz. by mixing small amounts of opposite-parity

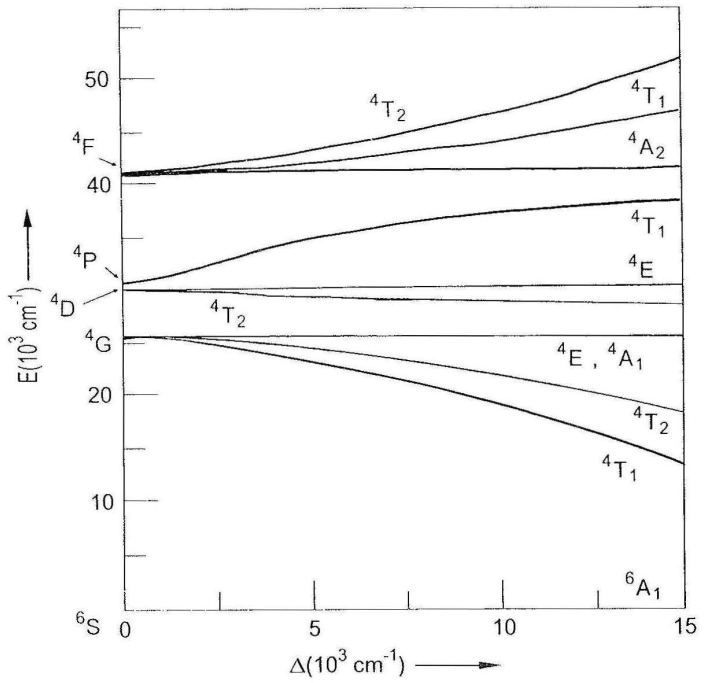

Fig. 2.10. The energy levels of the d^5 configuration as a function of the octahedral crystal field. The abscis is the ground state level ($^6S \rightarrow {}^6A_1$). Only the sextet and the quartets are given. Doublets are omitted for clarity

wave functions into the d wave functions [13]. Actually, the color of tetrahedrally coordinated transition-metal ions is not so weak as that of the octahedrally coordinated ones.

The more-electron cases are considerably more complicated (Figs 2.9 and 2.10). However, remembering the selection rules, we can derive the absorption spectra to be expected. For an ion with three $d$electrons, for example $Cr^{3+}(3d^3)$, the ground level is $^4A_2$. Optical absorption will, in good approximation, occur only to the spin-quartet ($2S + 1 = 4$) levels in view of the spin selection rule. There are only three of these transitions possible, viz. $^4A_2 \rightarrow {}^4T_2$, $^4T_1(^4F)$ and $^4T_1(^4P)$. Indeed the absorption spectrum of the Cr^{3+} ion consists of three absorption bands with low intensity (parity selection rule). This is shown in Fig. 2.12. The spin-forbidden transitions can usually be observed only in very accurate measurements.

The last example is the d^5 configuration, of which Mn^{2+}, used in many luminescent materials, is a well-known representative. The Tanabe-Sugano diagram is given in Fig. 2.10. In octahedral coordination the ground level is $^6A_1$. All optical absorption transitions are parity and spin forbidden. In fact the Mn^{2+} ion is practically colorless.

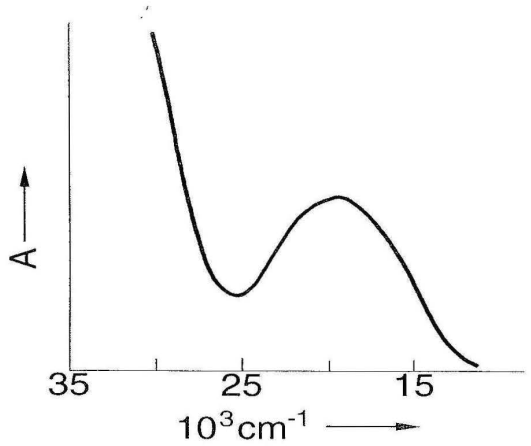

Fig. 2.11. The absorption spectrum of Ti^{3+} $(3d^1)$ in aqueous solution. The band at about 20000 cm^{-1} is the $^2T_2 \rightarrow {}^2E$ transition; the intense band in the ultraviolet is a charge-transfer transition

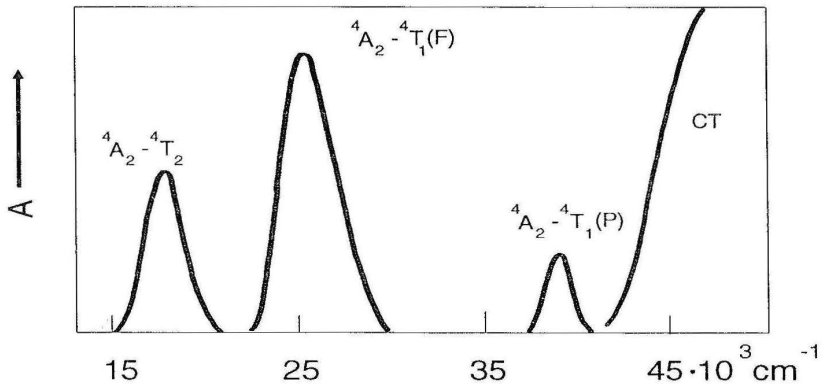

Fig. 2.12. Schematic representation of the absorption spectrum of Cr^{3+} $(3d^3)$ in an oxide. The spin-allowed crystal-field transitions are clearly visible. At high energy a charge-transfer (CT) transition occurs

However, Mn^{2+} compounds, like MnF_2 and $MnCl_2$, have a light rose color. The absorption spectrum of MnF_2 is given in Fig. 2.13. A large number of spin-sextet to spin-quartet transitions is observed, in agreement with Fig. 2.10. The molar absorption coefficient is two orders of magnitude lower than for Cr^{3+} in view of the spin selection rule. That for Cr^{3+} is more than three orders of magnitude lower than for allowed transitions (parity selection rule).

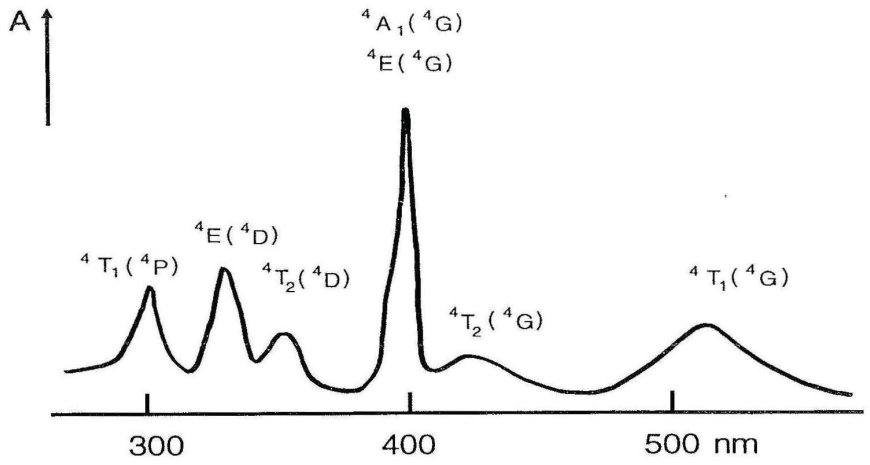

Fig. 2.13. Absorption spectrum of MnF_2

An interesting aspect of the absorption spectrum of Mn^{2+} is the different width of the absorption transitions. Especially the practically coinciding $^6A_1 \rightarrow {}^4A_1$ and ^4E bands are very narrow, and the $^6A_1 \rightarrow {}^4T_1$ and $^4T_2$ rather broad. Above it was shown that the band width is due to coupling with vibrations. Since the crystal field strength varies during the vibration, the Tanabe-Sugano diagrams also predict the width of the absorption bands. If the level reached after absorption runs parallel with the ground level (i.e. the x axis), a variation of Δ will not influence the transition energy, and a narrow absorption band is to be expected. If the excited level has a slope relative to the x axis, a variation of Δ will influence the transition energy, and a broad absorption band is to be expected. The reader can convince himself from the correctness of these statements by comparing Figs 2.11–13 with Figs 2.8–10.

The physical background of these statements was given above. Let us illustrate this for Mn^{2+}. The ground level configuration written in one-electron crystal-field components is $t_2{}^3e^2$. The excited $^4A_1$ and ^4E levels originate from the same configuration. Therefore ΔR is vanishing, and the transitions $^6A_1 \rightarrow {}^4A_1$ and ^4E should appear in the absorption spectrum as lines, in agreement with experiment. However, the levels $^4T_1$ and $^4T_2$ originate mainly from a different configuration, viz. $t_2{}^4e^1$. Since the chemical bond involving a t_2 orbital is different from that involving an e orbital, this configuration has an equilibrium distance which differs from that of the $t_2{}^3e^2$ ground configuration. Therefore, transitions like $^6A_1 \rightarrow {}^4T_1$ and $^4T_2$ involve a change in R_0 (i.e. $\Delta R \neq 0$) and should be observed in the spectra as bands with a certain width.

In the ultraviolet region the transition metal ions show usually broad and strong absorption bands due to ligand-to-metal charge-transfer transitions. These will be discussed now for the simple, but important case in which the d electrons are lacking.

This will be indicated here as a d^0 ion. Examples are Cr^{6+} and Mn^{7+} which are strongly colored in oxides (chromates, permanganates). This intense color is due to the fact that the charge-transfer transition has shifted into the visible. From the view point of luminescent materials, the more important examples are V^{5+} ($3d^0$), Nb^{5+} ($4d^0$) and W^{6+} ($5d^0$).

2.3.2 The Transition Metal Ions with d^0 Configuration

Compounds like YVO_4, $YNbO_4$ and $CaWO_4$ are very important materials in view of their luminescence properties. Their absorption spectra show strong and broad bands in the ultraviolet. The transition involved is a charge transfer from oxygen to the d^0 ion [14]. An electron is excited from a non-bonding orbital (on the oxygen ions) to an anti-bonding orbital (mainly $d$on the metal ion). Therefore the bonding is strongly weakened after optical absorption, so that $\Delta R >> 0$and the band width is large.

The spectral position of this absorption transition depends on many factors: the ionization potential of the $d^1 \rightarrow d^0$ ionization, the number and nature of the ligands, and the interaction between ions mutually in the lattice. Without further discussion the following examples are given by way of illustration:

- whereas $CaWO_4$ has the first absorption transition at 40 000 cm^{-1} (250 nm), $CaMoO_4$ has it at 34 000 cm^- (290 nm). This illustrates the higher sixth ionisation potential of Mo (70 eV) relative to W (61 eV), since all other factors are equal.
- whereas $CaWO_4$ with WO_4^{2-} groups has the first absorption transition at 40 000 cm^{-1}, that of Ca_3WO_6 with WO_6^{6-} groups is at 35 000 cm^{-1}, illustrating the shift of the charge-transfer band to lower energies if the number of ligands increases.
- whereas Ca_3WO_6, with isolated WO_6^{6-} groups, has its charge-transfer band at 35 000 cm^{-1}, that of WO_3, with WO_6^{6-} groups sharing oxygen ions, is in the visible (WO_3 is yellow colored); this illustrates the effect of interaction between optical centers with charge-transfer bands.

2.3.3 The Rare Earth Ions ($4f^n$)

The rare earth ions are characterised by an incompletely filled $4f$shell. The $4f$orbital lies inside the ion and is shielded from the surroundings by the filled $5s^2$ and $5p^6$ orbitals. Therefore the influence of the host lattice on the optical transitions within the $4f^n$ configuration is small (but essential). Figure 2.14 presents a substantial part of the energy levels originating from the $4f^n$ configuration as a function of n for the trivalent ions. The width of the bars in Fig. 2.14 gives the order of magnitude of the crystal field splitting which is seen to be very small in comparison with the transition metal ions.

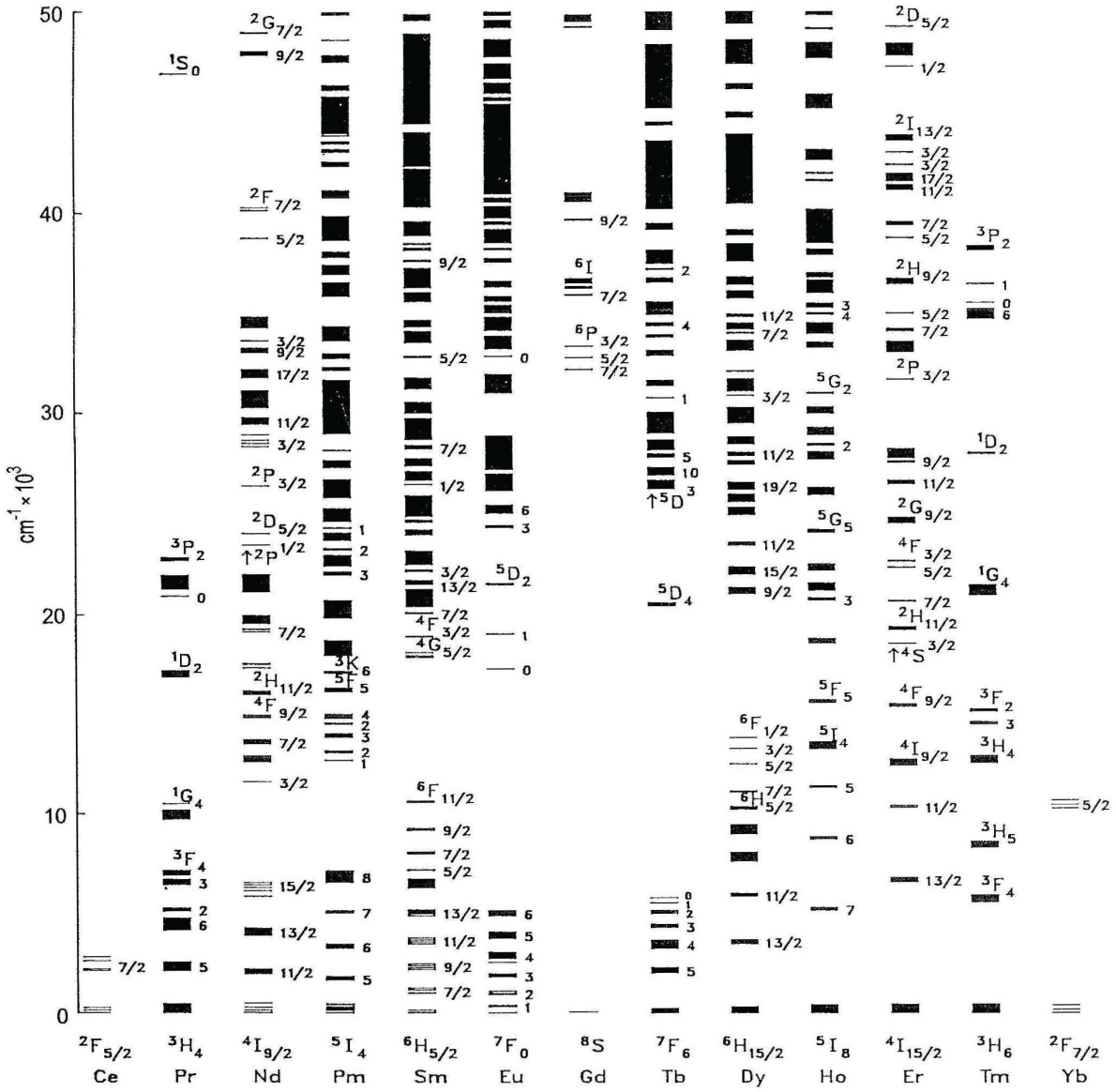

Fig. 2.14. Energy levels of the $4f^n$ configurations of the trivalent lanthanide ions (with permission reproduced from Carnall WT, Goodman GL, Rajnak K, Rana RS (1989) J Chem Phys 90: 343

Optical absorption transitions are strongly forbidden by the parity selection rule. Generally speaking the color of the oxides RE_2O_3 is close to white, although there are energy levels in the visible region. Only Nd_2O_3 (faint violet) is clearly colored. The dark colors of the commercial praseodymium and terbium oxides are due to the simultaneous presence of tri- and tetravalent ions (see below).

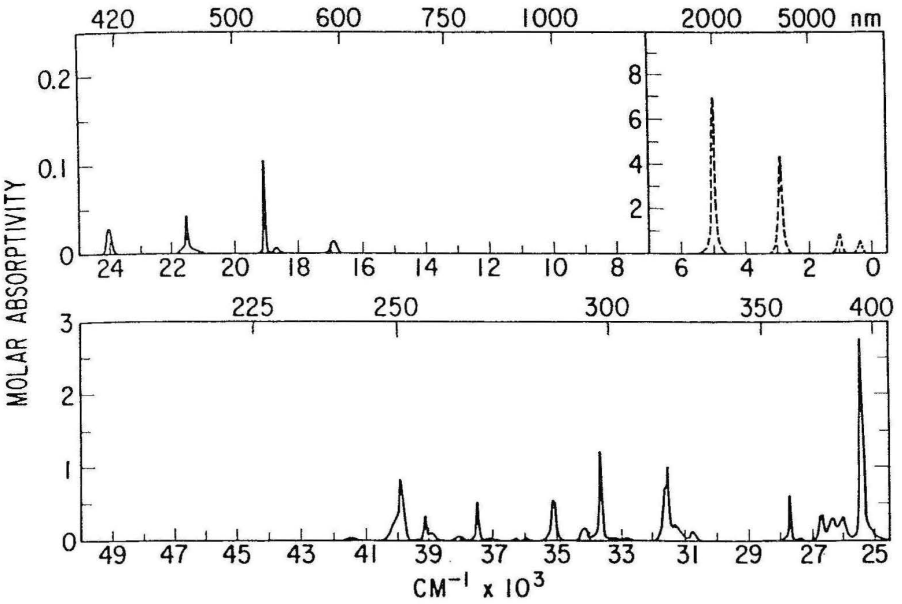

Fig. 2.15. Absorption spectrum of the Eu^{3+} ion in aqueous solution (with permission reproduced from Carnall WT (1979) Handbook on the physics and chemistry of rare earths, vol. 3. North Holland, Amsterdam, p. 171)

Figure 2.15 shows as an example the absorption spectrum of Eu^{3+} in aqueous solution. The sharpness of the lines has already been discussed before: for intraconfigurational $4f^n$ transitions $\Delta R = 0$. Note also the very low values of the molar absorption coefficient.

How is the parity selection rule relaxed? Vibrations have only a very weak influence. For interesting consequences of this influence the reader is referred to Ref. [15]. Of more importance are the uneven components of the crystal-field which are present when the rare earth ion occupies a crystallographic site without inversion symmetry. These uneven components mix a small amount of opposite-parity wave functions (like $5d$) into the $4f$ wavefunctions. In this way the intraconfigurational $4f^n$ transitions obtain at least some intensity. Spectroscopists say it in the following way: the (forbidden) $4f$-$4f$ transition steals some intensity from the (allowed) $4f$-$5d$ transition. The literature contains many treatments of these rare earth spectra, some in a simple way, others in considerable detail [1,16,17,18,19].

If the absorption spectra of the rare earth ions are measured at high enough energy, allowed transitions are also observed as will be discussed now.

2.3.4 The Rare Earth Ions ($4f$-$5d$ and Charge-Transfer Transitions)

The allowed optical transitions of the rare earth ions mentioned above are interconfigurational and consist of two different types, viz.

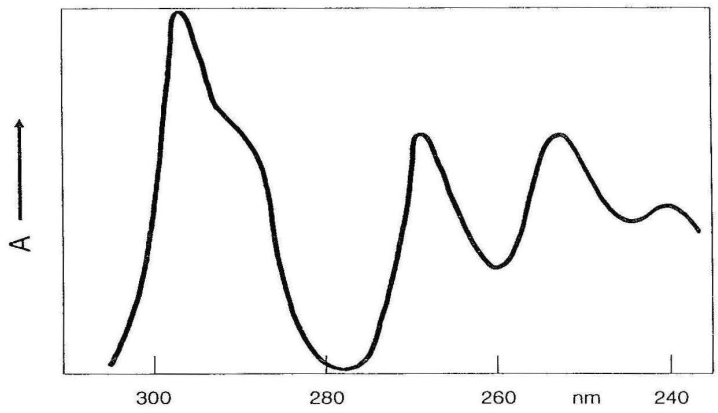

Fig. 2.16. Absorption spectrum of the Ce^{3+} ($4f^1$) ion in $CaSO_4$. The $4f \rightarrow 5d$ transition has five components due to the crystal-field splitting of the excited $5d$configuration

- charge-transfer transitions ($4f^n \rightarrow 4f^{n+1}L^{-1}$, where L = ligand)
- $4f^n \rightarrow 4f^{n-1}5d$ transitions.

Both are allowed, both have $\Delta R \neq 0$, and appear in the spectra as broad absorption bands. Charge transfer transitions are found for rare earth ions which like to be reduced, $4f$-$5d$transitions for ions which like to be oxidized. The tetravalent rare earth ions (Ce^{4+}, Pr^{4+}, Tb^{4+}) show charge-transfer absorption bands [20]. Orange $Y_2O_3 : Tb^{4+}$ has its color due to a charge-transfer absorption band in the visible.

The divalent rare earth ions (Sm^{2+}, Eu^{2+}, Yb^{2+}), on the other hand, show $4f \rightarrow 5d$ transitions, Sm^{2+} in the visible, Eu^{2+} and Yb^{2+} in the long wavelength ultraviolet.

The trivalent ions that have a tendency to become divalent (Sm^{3+}, Eu^{3+}, Yb^{3+}) show charge-transfer absorption bands in the ultraviolet. In the less electronegative sulfides also ions like Nd^{3+}, Dy^{3+}, Ho^{3+}, Er^{3+} and Tm^{3+} show charge-transfer transitions (in the spectral area around 30 000 cm^{-1}).

The trivalent ions that have a tendency to become tetravalent (Ce^{3+}, Pr^{3+}, Tb^{3+}) show $4f \rightarrow 5d$ absorption bands in the ultraviolet. An example is given in Fig. 2.16.

This type of optical transition is discussed in more detail in ref. [21].

2.3.5 Ions with s^2 Configuration

Ions with s^2 configuration show strong optical absorption in the ultraviolet due to a $s^2 \rightarrow sp$ transition (parity allowed). The s^2 configuration gives one level for the ground state, viz. $^1S_0$. The subscript indicates the value of J, the total angular momentum of the ion. The sp configuration yields, in sequence of increasing energy, the $^3P_0$, $^3P_1$, $^3P_2$, and $^1P_1$ levels.

In view of the spin selection rule the only optical absorption transition to be expected is $^1S_0 \rightarrow {}^1P_1$. Indeed this transition dominates the absorption spectrum (Fig. 2.17). However, the transition $^1S_0 \rightarrow {}^3P_1$ can also be observed. This is due to spin-orbit coupling which mixes the spin triplet and singlet, the more so for the

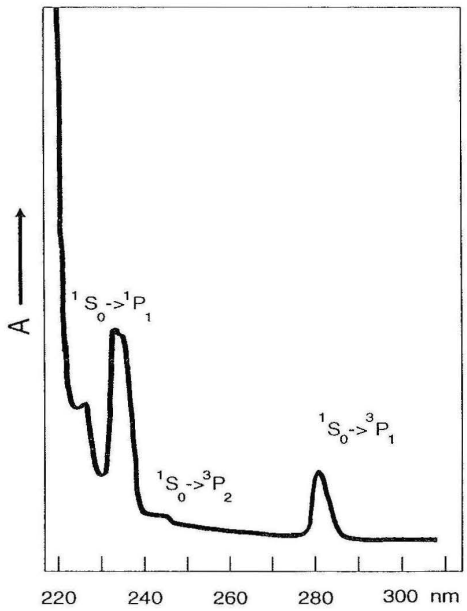

Fig. 2.17. Absorption spectrum of KI-Tl^+. The Tl^+ ion has $6s^2$ configuration. The transitions originating from the $6s^2 \rightarrow 6s6p$ transition are indicated. The absorption transitions at higher energy are due to charge transfer and the host lattice

heavier elements. Indeed the spin-forbidden transition becomes more intense in the series $As^{3+}(4s^2)$, $Sb^{3+}(5s^2)$, $Bi^{3+}(6s^2)$.

The transition $^1S_0 \rightarrow {}^3P_0$ remains forbidden, since the total angular momentum does not change ($\Delta J = 0$). The $^1S_0 \rightarrow {}^3P_2$ transition remains also forbidden ($\Delta J = 2$ is a forbidden transition), but can obtain some intensity by coupling with vibrations. For more details on the energy levels and transitions of s^2 ions, the reader is referred to Ref. [22].

Since bonding with p electrons is different from that with s electrons, $\Delta R \neq 0$, and broad absorption bands are to be expected. The band width of s^2 ions depends, however, strongly on the host lattice. This will be discussed in the next chapter.

2.3.6 Ions with d^{10} Configuration

Ions with d^{10} configuration like Zn^{2+}, Ga^{3+}, Sb^{5+}, etc. show an intense and broad absorption band in the short wavelength ultraviolet. In recent years it has become clear that such ions can also show luminescence [23]. The exact nature of the optical absorption transition is not clear, but it consists of a charge-transfer transition from the ligands ($2p$ orbital of oxygen) to an antibonding orbital which is situated partly on the d^{10} ion and partly on the ligands. In this way the large width and high intensity of the absorption band can be accounted for.

2.3.7 Other Charge-Transfer Transitions

Several examples of charge-transfer transitions have been given above. These were all of the LMCT (ligand-to-metal charge transfer) type. However, MLCT (metal-to-ligand charge transfer) is also possible, although in oxides not very probable. In coordination compounds these are quite common.

Another type is MMCT (metal-to-metal charge-transfer) [24,25] in which an electron is transferred from one metal ion to another. If the ions involved are of the same element, this is called intervalence charge-transfer. This occurs in Prussian blue which contains Fe^{2+} and Fe^{3+}, and $BaBiO_3$ with Bi^{3+} and Bi^{5+} ions. Examples where the metal ions are different are blue sapphire (Al_2O_3 : Fe^{2+},Ti^{4+}; the color is due to $Fe^{2+} \rightarrow Ti^{4+}$ charge transfer), YVO_4 : Bi^{3+} (with $Bi^{3+} \rightarrow V^{5+}$ charge transfer) and the luminescent material $CaWO_4$: Pb^{2+} (with $Pb^{2+} \rightarrow W^{6+}$ charge transfer).

As a matter of fact, all absorption bands due to this type of transitions are very broad.

2.3.8 Color Centers

The best-known color center is the F center. It consists of an electron in a halide vacancy in, for example, KCl. It occurs only in solids. In good approximation its absorption spectrum can be described in the same way as that of the hydrogen atom. The first optical transition is $1s \rightarrow 2p$ (parity allowed). In KCl its absorption maximum is in the red, so that a KCl crystal containing F centers is strongly blue colored.

The theory of these transitions is nowadays known in great detail. Many other color centers exist. Their treatment is outside the scope of this book. The reader is referred to Refs [1] and [2].

2.4 Host Lattice Absorption

As we have seen above, absorption of radiation does not necessarily take place in the luminescent center itself, but may also occur in the host lattice. It is obvious to make a simple subdivision into two classes of optical absorption transitions, viz. those which result in free charge carriers (electrons and holes), and those which do not. Photoconductivity measurements can distinguish between these two classes.

An example of the former class is ZnS, the host lattice for cathode-ray phosphors. This compound is a semiconductor. Optical absorption occurs for energies larger than E_g, the width of the forbidden gap. This absorption creates an electron in the conduction band and a hole in the valence band. Since the top of the valence band consists of levels with predominant sulfur character and the bottom of the conduction band of levels with a considerable amount of zinc character, the optical transition is of the charge transfer type. Its position can be shifted by replacing Zn and/or S in ZnS by other elements (see Table 2.3).

Table 2.3. Somesemiconductors of the ZnS type and their optical absorption.

	E_g (eV)	color
ZnS	3.90	white
ZnSe	2.80	orange
ZnTe	2.38	red
CdS	2.58	orange
CdTe	1.59	black

However, not every host lattice yields free electrons and holes upon optical excitation. Ultraviolet irradiation of $CaWO_4$, for example, is absorbed in the WO_4^{2-} groups as described above. In the excited state of the tungstate group the hole (on oxygen) and the electron (on the tungsten) remain together: their interaction energy is strong enough to prevent delocalisation like in ZnS. Such a bound electron-hole pair is called an exciton, and more specifically when the binding is strong, as in $CaWO_4$, a Frenkel exciton [1,26]. Another example is the first absorption band of NaCl, situated at 8eV (155 nm) in the vacuum ultraviolet. It is due to the $3p^6 \rightarrow 3p^5 4s$ transition on the Cl^- ion. Strongly coupled electron-hole pairs occur only in ionic compounds.

The processes occurring upon irradiating a material with high-energy radiation like cathode rays, X rays or γ rays are rather complicated. After penetration into the solid, this radiation will give ionisation depending on the type and the energy of the radiation. This ionisation creates many secondary electrons. After thermalisation we are left with electron-hole pairs, as we do after irradiation with ultraviolet radiation just over the band gap.

We have described in this chapter the processes and transitions which are responsible for the absorption of radiation, with special attention to ultraviolet radiation and absorption by the center itself. Our systems are now in the excited state. In the following chapters we will consider how they return again to the ground state. Sometimes they follow simply the reverse of the absorption transition, but more often they prefer a different way without hesitating to make large detours.

References

1. Henderson B, Imbusch GF (1989) Optical spectroscopy of inorganic solids. Clarendon, Oxford
2. Stoneham AM (1985) Theory of defects in solids. Clarendon, Oxford.
3 DiBartolo B (1968) Optical interactions in solids. Wiley, New York
4. Atkins PW (1990) Physical chemistry, 4th edn. Oxford University Press, Oxford
5. Jørgensen CK (1962) Absorption spectra and chemical bonding in complexes. Pergamon, Oxford
6. Jørgensen CK (1971) Modern aspects of ligand field theory, North-Holland, Amsterdam
7. Lever ABP (1984) Inorganic electronic spectroscopy, 2nd edn. Elsevier, Amsterdam
8. Duffy JA (1990) Bonding, energy levels and bands in inorganic solids. Longman Scientific and Technical, Harlow
9. Blasse G (1972) J Solid State Chem 4: 52

10. Antic-Fidancev E, Lemaitre-Blaise M, Derouet J, Latourette B, Caro P (1982) C.R. Ac. Sci. Paris 294: 1077
11. Flahaut J (1979) Ch. 31 in Vol. 4 of the Handbook on the physics and chemistry of rare earths, North-Holland, Amsterdam
12. Shriver DF, Atkins PW, Langford CH (1990) Inorganic Chemistry, Oxford University Press, Oxford
13. Cotton FA (1990) Chemical Applications of Group Theory, 3rd edn. Wiley, Chichesterter
14. Blasse G (1980) Structure and Bonding 42: 1
15. Blasse G (1992) Int. Revs Phys. Chem. 11: 71
16. Judd BR (1962) Phys. Rev. 127: 750; Ofelt GS (1962) J. Chem. Phys. 37: 511
17. Carnall WT (1979) Chapter 24 in vol. 3 of the Handbook on the physics and chemistry of rare earths (Gschneidner KA Jr, Eyring L eds) North-Holland Amsterdam
18. Blasse G (1979) Chapter 34 in vol. 4 of the Handbook on the physics and chemistry of rare earths (Gschneidner KA Jr, Eyring L eds) North-Holland Amsterdam; (1987) Spectroscopy of solid-state laser-type materials (DiBartolo B. ed.) Plenum New York (1987) 179
19. Peacock RD (1975) Structure and Bonding 22: 83
20. Hoefdraad HE (1975) J. Inorg. Nucl. Chem. 37: 1917
21. Blasse G (1976) Structure and Bonding 26: 43
22. Ranfagni A, Mugnai D, Bacci M, Viliani G, Fontana MP (1983) Adv. Physics 32: 823
23. Blasse G (1990) Chem. Phys. Letters 175: 237
24. Blasse G (1991) Structure and Bonding 86: 153
25. Brown DB (ed.) (1980) Mixed-valence compounds, Reidel, Dordrecht
26. Kittel C, Introduction to solid state physics, Wiley, New York, several editions.

CHAPTER 3

Radiative Return to the Ground State: Emission

3.1 Introduction

In Chapter 2, several ways were considered in which the luminescent system can absorb the excitation energy. In the following chapters the several possibilities of returning to the ground state are considered. In this chapter we will deal with radiative return to the ground state in the case when the absorption and emission processes occur in the same luminescent center. This situation occurs when photoluminescence is studied on a luminescent center in low concentration in a non-absorbing host lattice (Fig. 1.1).

In Chapter 4 nonradiative return to the ground state will be discussed for a comparable situation. Chapter 5 deals with another possibility of returning to the ground state, viz. transfer of the excitation energy of one ion to another (Fig. 1.3).

This chapter is organized as follows. First a general discussion will be given on the basis of the configurational coordinate diagram (see Chapter 2). Then we will consider a number of different classes of luminescent ions. At the end some special effects, like afterglow and stimulated emission, are treated.

3.2 General Discussion of Emission from a Luminescent Center

Figure 3.1 shows again the configurational coordinate diagram. For the moment we assume that there is an offset between the parabolas of the ground and excited state. According to Chapter 2 absorption occurs in a broad optical band and brings the center in a high vibrational level of the excited state. The center returns first to the lowest vibrational level of the excited state giving up the excess energy to the surroundings. Another way to describe this process is to say that the nuclei adjust their positions to the new (excited) situation, so that the interatomic distances equal the equilibrium distances belonging to the excited state. The configurational coordinate changes by ΔR. This process is called relaxation.

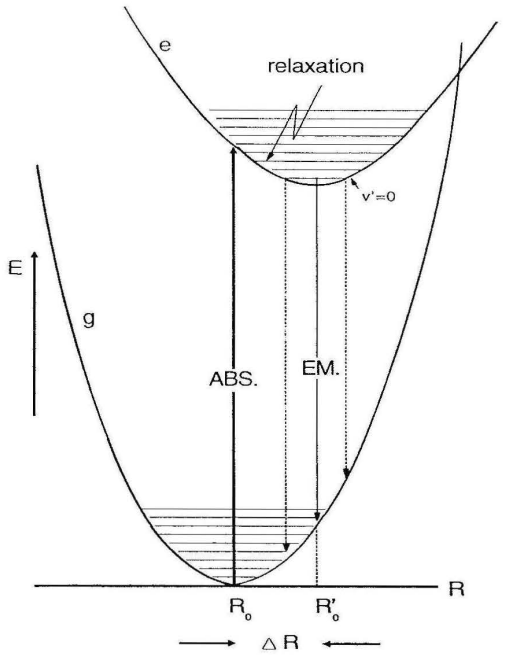

Fig. 3.1. Configurational coordinate diagram (see also Fig. 2.3). The absorption transition g → e is for reasons of clarity drawn as one line only (the transition with maximum intensity). After absorption the system reaches high vibrational levels of the excited state. Subsequently it relaxes to the lowest vibrational level $v' = 0$ from where emission e → g occurs in a broad band. The parabola offset is given by ΔR

During relaxation there occurs usually no emission, and certainly not of high intensity. This can be easily seen from the rates involved: whereas a very fast emission has a rate of 10^8 s^{-1}, the vibrational rate is about 10^{13} s^{-1}.

From the lowest vibrational level of the excited state the system can return to the ground state spontaneously under emission of radiation. The rules for this process are the same as described for the absorption process. The difference is that emission occurs spontaneously (i.e. in the absence of a radiation field), whereas absorption can only occur when a radiation field is present. The reverse process of absorption is stimulated emission (see Sect. 3.6) and not spontaneous emission.

By emission, the center reaches a high vibrational level of the ground state. Again relaxation occurs, but now to the lowest vibrational level of the ground state. The emission occurs at a lower energy than the absorption due to the relaxation processes (see Fig. 3.1). As an example, Figure 3.2 shows the emission and excitation (= absorption) spectra of the luminescence of Bi^{3+} in LaOCl. The energy difference between the maximum of the (lowest) excitation band and that of the emission band is called the Stokes shift. It will be immediately clear that the larger the value of ΔR is, the larger the Stokes shift and the broader the optical bands involved.

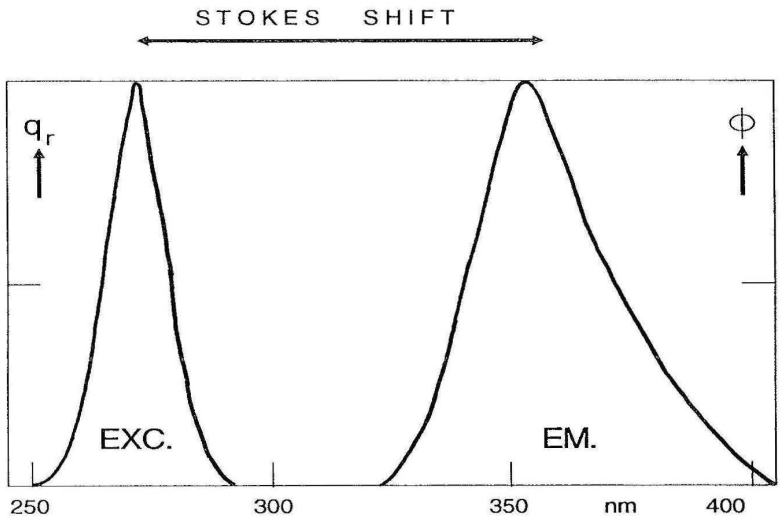

Fig. 3.2. Emission and excitation spectra of the Bi^{3+} luminescence of $LaOCl : Bi^{3+}$. The Stokes shift amounts to about 9000 cm^{-1}. In this and other figures q_r gives the relative quantum output and Φ the spectral radiant power per constant wavelength interval, both in arbitrary units

If the two parabolas have equal force constants (i.e. the same shape), the amount of energy lost in the relaxation process is $Sh\nu$ per parabola, where $h\nu$ is the spacing between two vibrational levels and S an integer. The Stokes shift amounts to $2Sh\nu$. The constant S is called the Huang-Rhys coupling constant. It is proportional to $(\Delta R)^2$ (see e.g. Ref. [1] and measures the strength of the electron-lattice coupling. If $S < 1$, we are in the weak-coupling regime, if $1 < S < 5$, in the intermediate coupling regime, if $S > 5$, in the strong-coupling regime.

If R denotes the distance between the central metal ion and the ligands, the absorption-emission cycle can be visualized as follows: absorption occurs without change of R, and is followed by expansion of the luminescent center till the new equilibrium distance $(R + \Delta R)$ is reached; subsequently emission occurs without change of distance followed by a contraction ΔR till the equilibrium distance of the ground state is reached. This is a classic description which, however, is often not correct, since the excited state may be distorted relative to the ground state.

As an example of such a distortion we consider the Te^{4+} ion [2]. In a composition like $Cs_2SnCl_6 : Te^{4+}$ this ion shows a yellow luminescence (see Fig. 3.3). The value of the Stokes shift is 7000 cm^{-1}. The emission spectrum shows a clear structure (Fig. 3.3) which consists of a large number of equidistant lines. Their energy difference is 240 cm^{-1}. It corresponds to a vibrational mode of the ground state. From Raman spectra it can be derived that this vibrational mode is not the one in which all metal-ligands bonds expand and contract in phase (ν_1). The 240 cm^{-1} mode is a mode in which the luminescent $TeCl_6^{2-}$ octahedron is tetragonally distorted (ν_2) (Fig. 3.4). The configurational coordinate to be taken is ν_2. This means that the $TeCl_6^{2-}$ octahedron is tetragonally distorted during the relaxation after optical absorption. After emission

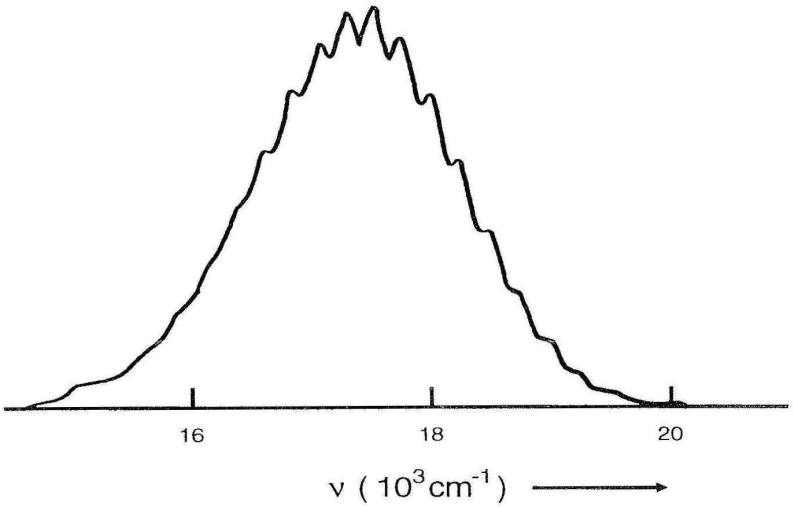

Fig. 3.3. Emission spectrum of $Cs_2SnCl_6 : Te^{4+}$ at 4.2 K

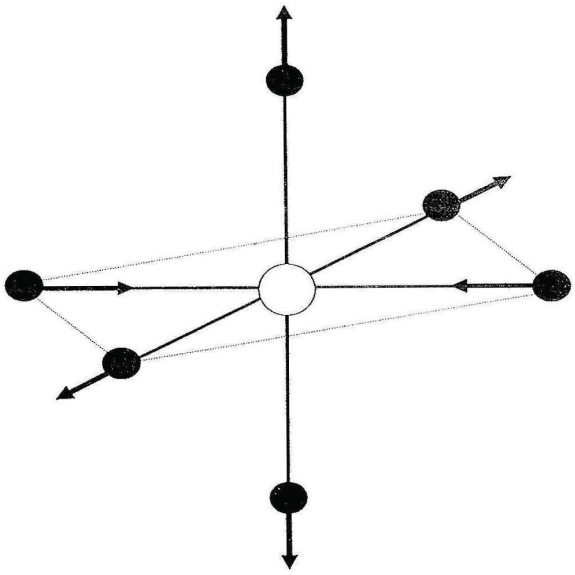

Fig. 3.4. The vibrational ν_2 mode of the octahedron ML_6 (M = metal ion, L : ligand ion)

it relaxes to the undistorted ground state. Similar results have been reported for Cr^{3+} in CrO_6^{9-} and the vanadate group (VO_4^{3-}) (see below).

As a matter of fact the coupling with all possible vibrational modes has to be considered. Fortunately the coupling with only one mode dominates in many cases, i.e. the coupling constant S is small for all modes except this one. Analysis is then

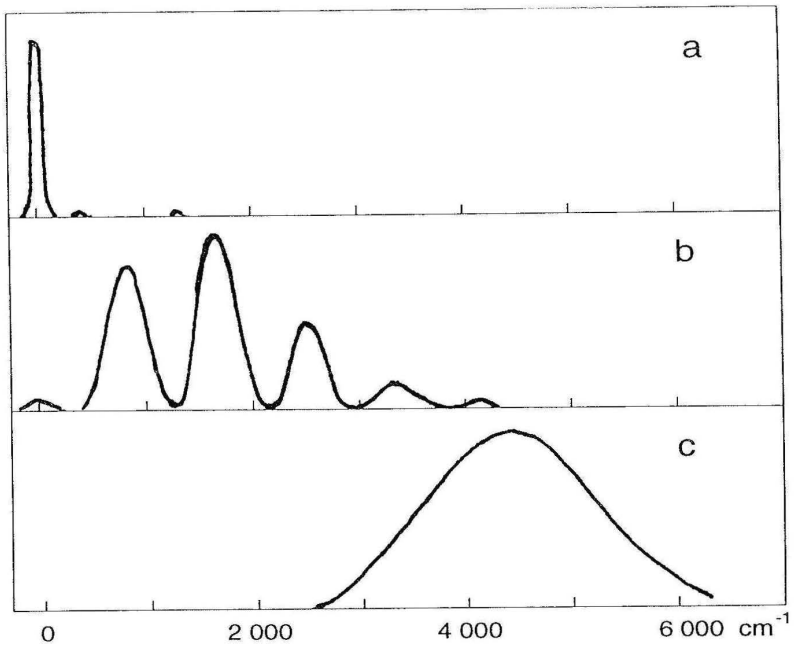

Fig. 3.5. Emission spectra at low temperature of $GdAl_3B_4O_{12}$ (*a*), UO_2^{2+} (*b*), and the F centre. The position of the zero-phonon line is always at 0 cm^{-1}. In (*a*) the zero-phonon line dominates (Gd^{3+}, $S \sim 0$), in (*b*) it is still observable ($S \sim 2$), and in (*c*) it has vanished ($S > 5$). The absolute position of the emission is for (*a*) in the ultraviolet, for (*b*) in the green, and for (*c*) in the infrared

possible. If coupling with several modes is effective, the spectral band is broad and the amount of information which can be obtained from it decreases rapidly.

For the emission band shape the same considerations are valid as for the absorption band shape (Chapter 2). Figure 3.5 shows a few emission spectra of different luminescent species, viz. Gd^{3+}, UO_2^{2+} and the F center. These spectra are plotted on the same energy scale and relative to the zero-phonon line. In the case of Gd^{3+} the zero-phonon line dominates (weak coupling), in the case of UO_2^{2+} there is a clear progression in the ν_1 mode (the symmetrical stretching mode; intermediate coupling); in the case of the F center there is a broad band and the intensity of the zero-phonon line has vanished (strong coupling). It is the nature of the luminescent species which determines the value of S (the strength of the electron-lattice coupling).

Nevertheless, there is also an influence of the host lattice. For example, Te^{4+} in Cs_2SnCl_6 shows an emission spectrum in which vibrational structure can be observed (Fig. 3.3). In $ZrP_2O_7 : Te^{4+}$, however, this structure has disappeared and the emission band width has more than doubled. The Bi^{3+} ion shows vibrational structure in its emission band in $ScBO_3$, but not in $LaBO_3$ [3]. The disappearance of the vibrational structure points to an increase of the value of S or of the offset ΔR. It has been shown that a stiff surroundings of the luminescent center restricts the value of ΔR and of S, so that the Stokes shift becomes smaller and vibrational structure may appear in

favourable cases. The influence of this stiffness is even more pronounced in the case of processes which enable nonradiative return to the ground state (see Chapter 4).

The influence of the host lattice on the absorption transitions (Chapter 2) is of course also present in the case of emission transitions. This influence is different from the influence of the host lattice on ΔR and S, so that the influence of the host lattice on the emission transition is not easy to unravel: the influence of several effects has to be distinguished, and this is not always easy.

Whereas in absorption spectroscopy the strength of the optical absorption is measured in an easy and classic way [4], this is different in the case of emission spectroscopy. Here the key property is the life time of the excited state. For allowed emission transitions this life time is short, viz. $10^{-7} - 10^{-8}$ s, for strongly forbidden transitions in solids it is much longer, viz. a few 10^{-3} s. This life time is of great importance in many applications. Therefore we discuss this quantity in more detail. For the two-level system of Figure 3.1 (excited state and ground state) the population of the excited state decreases according to

$$\frac{dN_e}{dt} = -N_e P_{eg} \tag{3.1}$$

In Eq. (3.1) the value of N_e gives the number of luminescent ions in the excited state after an excitation pulse, t the time, and P_{eg} the probability for spontaneous emission from the excited to the ground state.

Integration yields

$$N_e(t) = N_e(0)e^{-P_{eg}t} \tag{3.2}$$

which is also written as

$$N_e(t) = N_e(0)e^{-t/\tau_R} \tag{3.3}$$

where $\tau_R (= P_{eg}^{-1})$ is the radiative decay time. A plot of the logarithm of the intensity versus time should give a linear curve. An example is given in Figure 3.6. After a time τ_R the population of the excited state has decreased to $\frac{1}{e}$ (37%).

The expression (2.1) is of course also valid for the emission transition. As for absorption transitions, the nuclear part determines the emission band shape. The electronic part determines the value of the radiative decay time.

The general knowledge discussed in this paragraph will now be illustrated by and applied on several classes of luminescent centers.

3.3 Some Special Classes of Luminescent Centers

3.3.1 Exciton Emission from Alkali Halides

This section starts with the alkali halides, because the intrinsic luminescent center in these compounds shows a complicated relaxation in the excited state which has